UNIVERSIDAD DE LA LAGUNA
FACULTAD DE CIENCIAS

TRABAJO DE FIN DE GRADO

Introduction to the analysis of systems in interaction with thermal baths: Langevin approach

José Antonio Almanza Marrero

Tutor: Antonia Ruiz García

Grado en Física

Curso académico 2020-2021

Convocatoria de Julio

Agradecimientos

Resumen

Este trabajo se plantea como una introducción al estudio de la dinámica de sistemas que se encuentran en interacción con baños térmicos. Abordaremos dos escenarios: la interacción con un único baño térmico, y la interacción con dos baños térmicos distintos. En el primer escenario el sistema evoluciona hasta alcanzar un estado estacionario de equilibrio térmico con el baño. Mientras que en el segundo escenario la acción combinada de los distintos baños determina la evolución del sistema hacia un estado estacionario de no equilibrio en el que emergen propiedades de transporte, caracterizadas por corrientes de calor entre los baños y el sistema.

En el caso de la interacción con un único baño consideramos sistemas sencillos en los que es posible hacer una resolución analítica de la dinámica. Abordaremos además la resolución numérica de las ecuaciones diferenciales estocásticas que describen dicha dinámica. Mostraremos el buen acuerdo alcanzado entre los resultados numéricos y analíticos. El análisis de sistemas en interacción con distintos baños térmicos se realizará principalmente en base a la resolución numérica de la dinámica.

Comenzamos nuestro estudio introduciendo todo el formalismo necesario para la descripción del movimiento browniano dentro del marco teórico empleado. Dicho marco lo proporciona la descripción de Langevin, en este modelo la acción del baño térmico se traduce en dos términos de características bien diferenciadas. Por un lado tenemos el término de fricción describiendo que la asimetría del acoplamiento entre unos pocos grados de libertad lentos y muchos rápidos conduce a un flujo de energía del primero al segundo, que es el fenómeno de la disipación de energía [1]. En contraposición, está el término conocido como fuerza estocástica o fuerza de langevin que da cuenta de las incesantes colisiones que sufre la partícula browniana con aquellas del medio que la rodea.

Una vez establecidos los fundamentos teóricos pasamos a la resolución de algunos casos particulares de sistemas que alcanzan el equilibrio donde vemos como se caracterizan estos estados, se presentan métodos alternativos para la solución de la dinámica del sistema y se comprueba la concordancia de los resultados analíticos que se van obteniendo con las simulaciones numéricas llevadas a cabo.

Por último, pasamos al estudio de sistemas fuera del equilibrio donde introducimos el concepto de equilibrio térmico local, un resultado que nos permite extrapolar consideraciones propias de sistemas en equilibrio a sistemas fuera de él. Basándonos en esto, caracterizamos la temperatura y los flujos de energía que aparecen en el sistema.

Introduction

Abstract

Este trabajo se presenta como una introducción al estudio de la dinámica de sistemas en contacto con baños térmicos en el marco teórico del modelo de Langevin. En dicho marco, tanto sistemas dentro como fuera del equilibrio son estudiados.

Aunque solo estudiamos modelos muy sencillos, entender los resultados que se mostrarán a continuación proporciona las herramientas necesarias para realizar estudios más complejos, ya sea aumentando el número de partículas del sistema o considerando otro tipo de potenciales de interacción. En sistemas de estas características fenómenos de transporte anómalos emergen.

This work is presented as an introduction to the study of the dynamics of systems in contact with thermal baths in the theoretical framework of the Langevin model. In this framework, both systems in and out of equilibrium will be studied. Characterizing them based on the values of the kurtosis of their velocity distribution.

Although we only study very simple models, understanding the results that will be shown below would provide the necessary tools to carry out more complex studies. Either increasing the number of particles in the system or considering other types of interaction potentials. In systems of these characteristics anomalous transport phenomena emerge. [2] [3]

In chapter one we start by introducing the basic concepts necessary to characterize stochastic processes, which are then applied to the specific case of Brownian motion. We also explain the Langevin model, which will be used to define the thermal baths in this study.

In chapter two we focus on systems that are in contact with a single thermal bath. These systems reach equilibrium when sufficient time has elapsed. Here we will study the behaviour of the mean values of the different dynamic quantities of the particle in the transition regime to equilibrium and once equilibrium has been reached. We analyze two systems: a free particle and a particle confined in an harmonic potential. In this case it is possible to find the analytical solution of the dynamics.

Chapter three is devoted to the study of systems that are in contact different thermal bath. In this case the combined action of different thermal baths determines the steady state to be non-equilibrium. We characterise such states in terms of the kurtosis and introduce the concept of local thermal equilibrium (LTE).

Although for such systems it becomes almost impossible to obtain analytical solutions, we show a semi-analytical method that allows us to analyse the state of the system once it is in the non-equilibrium steady state.

The Einstein approach to Brownian motion, the proof of the Central Limit Theorem and the description of the Platen‘s algorithm for the numerical resolution of the dynamical equations are presented on the appendix.

Contents

Chapter 1

Brownian motion.

Abstract

Comenzamos con este capítulo donde se introducen los conceptos básicos necesarios para definir procesos estocásticos, y que luego se aplican al caso concreto del movimiento browniano.

También se explica en qué consiste el modelo de Langevin, modelo que será empleado para definir los baños térmicos en este estudio.

In 1827 the botanist Brown discovered under his microscope vigorous irregular motion of small particles originating from pollen floating on water (Figure 1.1). *He also observed that very fine particles of minerals undergo similar incessant motion as if they were living objects. This discovery must have been a great wonder at that time. The idea of combining such a motion - Brownian motion - with molecular motion became fairly widespread in the latter half of the nineteenth century when atomism had not yet been fully recognized as reality. It was the celebrated work of Einstein, which appeared in 1905, that gave the first clear theoretical explanation of such a phenomenon which could be directly verified quantitatively by experiments and thus established the very basic foundation of the atomic theory of matter.*kubo (Einstein approach it´s shown on the Appendix A)

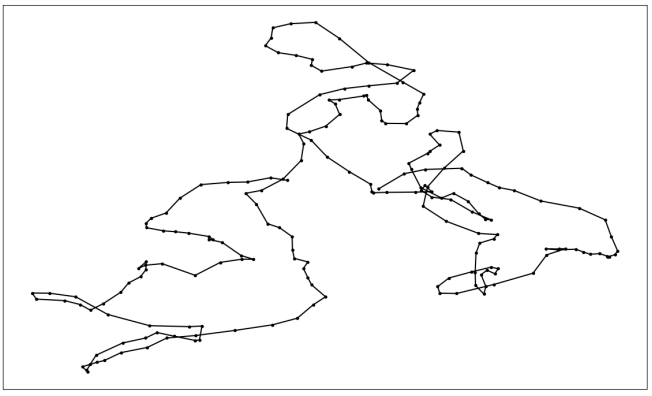

Figure 1.1: A typical trajectory of a particle undergoing Brownian motion.

1.1 Brownian motion as a Stochastic Process.

Suppose that we observe a Brownian particle over a time interval $0 < t < T$ *and obtain a record of its position* $x(t)$ *as a function of time. For simplicity we are going to consider only the projection on the* x *axis, but the essentials are the same for two or three dimensional motion. This observations are repeated in time to get* N *readings of the particle position*

$$x_1(t), x_2(t), ..., x_N(t).$$

These readings are all different, that is, the motion of the Brownian particle is not reproducible.[4]

So we must ask ourselves the question, "how can physics predict that motion?". Firstly, unlike in classic mechanics, we are not able to make deterministic descriptions of the motion, we must take a probabilistic outlook. *The value of the displacement* $x(t)$ *of the Brownian particle at time* t *is probabilistic and each of the observed* $x_i(t)$ *is a sample form a statistical ensemble. If we repeat the observations a great many times to make* N *very large, we should be able to find empirically the distribution law obeyed by* $x(t)$.[4]

A stochastic variable $X(t)$ is a series of random variables having t as a parameter. The time series of random variables is called *stochastic process*. With a large enough number of observations we can make a function $x(t)$ continuous with time t as a parameter that is a realization of the process. If observations are made at discrete times

$$0 < t_1 < t_2 ... < t_n < T$$

then a set of n real numbers

$$x(t_1), x(t_2), ..., x(t_n)$$

is a sample obtained by the observations.*If we regard the set as a vector, then an* n*-dimensional real space* R^n *is the sample space of the process* $X(t)$ *for the selected time points. An element of the sample space may also be represented by zig-zag path* (Figure 1). *One may consider the limit of very large* n *and vanishing lengths of time segments to attain a path with a continuous time. This is an intuitive conclusion, not easily made rigorous mathematically.*[4] In fact, a very rigorous mathematics is needed to define the adequate measure in the space consisting of the possible paths $x(t)$. Although this may be interesting from a theoretical-mathematical point of view, it is outside the scope of this work. Since we are interested in focusing on the physical aspects.

In understanding Brownian motion as such a stochastic process, how can $x(t)$ *be described in terms of probably theory? Firstly, what is the probability of finding an observed value* $x(t)$ *of* $X(t)$ *at time* t *in the interval between* x *and* $x + dx$*?*[4] If its probability density is W_1, then the probability is

$$W_1(x, t)dx = Pr(x < x(t) < x + dx). \tag{1.1}$$

On the right-hand side, $Pr(...)$ means the probability of the event in the curly bracket occurring. *Next, what is the probability that two observed values* $x(t_1)$ *and* $x(t_2)$ *at times* t_1 *and* t_2 *are found in the intervals* $(x_1, x_1 + dx_1)$ *and* $(x_2, x_2 + dx_2)$*, respectively?*[4] In this case, the probability density W_2 is defined by

$$W_2(x_1, t_1; x_2, t_2)dx_1dx_2 = Pr(x_1 < x(t_1) < x_1 + dx_1, x_2 < x(t_2) < x_2 + dx_2). \tag{1.2}$$

More generally, for a set of observed values $x(t_1), x(t_2), ..., x(t_n)$ at $t_1, t_2, ...$ and t_n

$$W_n(x_1, t_1; x_2, t_2; ...; x_n, t_n)dx_1dx_2...dx_n = Pr(x_i < x(t_i) < x_i + dx_i, i = 1, 2, ..., n). \quad (1.3)$$

This is the joint probability distribution for n random variables, $X(t_1), X(t_2), ...,$ and $X(t_n)$. *The stochastic process $X(t)$ is defined when such probabilities are given for any set of n ($n = 1, 2, .., \infty$) time points. In other words, each possible path of the Brownian motion $x(t)$ has a probability assigned to it so that the probability (1.3) is defined as the sum of these probabilities for all possible paths going through the gates $dx_1, dx_2, ..., dx_n$ set at the selected time points.*[4]

Many kinds of probabilities can be derived from definitions (1.1-1.3). Particularly important is the conditional probability, which is defined as the probability that the Brownian particle is found at time t_1 between x_1 and $x_1 + dx_1$ when it was at x_0 at time t_0:

$$P(x_0, t_0|x_1, t_1)dx_1 = \frac{W_2(x_0, t_0; x_1, t_1)dx_1}{W_1(x_0, t_0)}. \quad (1.4)$$

Conditional probability for two time points are most commonly used, but a more general definition of conditional probabilities is

$$P(x_0, t_0|x_1, t_1; ...; x_n, t_n)dx_1...dx_n = \frac{W_{n+1}(x_0, t_0; x_1, t_1; ...; x_n, t_n)dx_1...dx_n}{W_1(x_0, t_0)} \quad (1.5)$$

for n observations at n time points when the initial state x_0 is precisely defined at time t_0.

1.2 The Central Limit Theorem.

The probability distribution of the displacement $X = x - x_0$ over the time interval $(0, t)$ obtained on the Appendix A is a normal distribution, or a Gaussian distribution, and its variance grows in proportion to time:

$$\langle X^2 \rangle = 2Dt. \quad (1.6)$$

Now the time interval is divided into n ($\gg 1$) segments Δt_i ($i = 1, 2, ..., n$) and displacements in each segment are denoted by ΔX_i. Then naturally

$$X = \sum_{i=1}^{n} \Delta X_i \quad and \quad \langle \Delta X_i \rangle = 0. \quad (1.7)$$

The expectation of the total displacement is zero

$$\langle X \rangle = 0. \quad (1.8)$$

Further, displacement in different time segments are statistically independent

$$\langle \Delta X_i \Delta X_j \rangle = 0 \quad (i \neq j)$$

.

Therefore it follows form (1.7) that

$$\langle X^2 \rangle = \sum_{i=1}^{n} \langle \Delta X_i^2 \rangle. \quad (1.9)$$

Taking equal lengths for the time segments $\langle \Delta X_i^2 \rangle$ we have

$$\langle X^2 \rangle = n \langle \Delta X^2 \rangle = t \frac{\langle \Delta X^2 \rangle}{\Delta t}. \tag{1.10}$$

Comparing with equation (1.6) tells us that the diffusion constant will fulfill a relation like

$$D = \frac{\langle \Delta X^2 \rangle}{2\Delta t} \tag{1.11}$$

The result (1.11) is simply a repetition of (1.6) but it has a deeper interpretation.

The well-known Gaussian law of errors teaches us that an observation error X follows a normal distribution if the error is an accumulation of a large number of small errors. The displacement X of Brownian particle is also a sum of a large number of successive small displacements ΔX_i. Therefore, we should expect that the distribution law of displacement X over a sufficiently long time interval t is normal.[4]

The Gaussian law of errors is contained in a very general theorem of probability theory called the *central limit theorem*, which is of fundamental importance in statistical physics. We are going to state it in a general way. Like for (1.7), we consider a sum of n ($\gg 1$) independent random variables $\Delta X_1, \Delta X_2, ..., \Delta X_n$ and we define

$$X_n = \Delta X_1 + \Delta X_2 + ... + \Delta X_n. \tag{1.12}$$

Here $\Delta X_1, \Delta X_2, ...$ and ΔX_n are assumed to have zero mean values as (1.7) and the variances

$$\langle \Delta X_j^2 \rangle = \sigma_j^2. \tag{1.13}$$

We set

$$s_n^2 = \sigma_1^2 + \sigma_2^2 + ... + \sigma_n^2. \tag{1.14}$$

The central limit theorem states that the probability distribution of the random variable

$$Y_n = \frac{X_n}{s_n} \tag{1.15}$$

tends to a normal distribution whose variance is equal to 1, which means that its distribution density $f_n(Y_n)$ will approach $f(Y)$ as

$$f_n(Y) \to \frac{1}{\sqrt{2\pi}} exp\left(-\frac{1}{2}Y^2\right) \tag{1.16}$$

asymptotically as n increases to infinity. It can be stated that the probability distribution density $P(X_n)$ of X_n has the form

$$P(X_n) \approx \frac{1}{\sqrt{2\pi s_n}} exp\left(-\frac{X_n^2}{2s_n^2}\right) \quad (n \gg 1). \tag{1.17}$$

The validity of the central limit theorem is determined because the n random variables $\Delta X_1, \Delta X_2, ...$ and ΔX_n are equally considered that there are not some that dominate the others. The demonstration of the theorem its given on the Appendix B.

1.3 The Langevin Equation.

So far we have concentrated on the displacement of Brownian particles. However, the physical model should start from the motion itself. The equation of motion of a particle with mass m is

$$m\frac{d\mathbf{v}}{dt} = \mathbf{F}, \tag{1.18}$$

where $\boldsymbol{v}$ is the velocity and $\boldsymbol{F}$ the force acting on the particle from molecules of the fluid surrounding the Brownian particle.

The force $\boldsymbol{F}$ may be divided into two parts. The first part is the frictional force, which is given in terms of the frictional coefficient γ, as

$$\mathbf{F}_v = -m\gamma\mathbf{v}. \tag{1.19}$$

The second part of the force is the reminder of the force, $\boldsymbol{F_v}$ subtracted from $\boldsymbol{F}$, and is regarded as random, independent of the motion of the particle. This part is called the random force or Langevin force and is hereafter denoted as $\boldsymbol{\xi}(t)$.

Then (1.18) can be written as

$$m\frac{d\mathbf{v}}{dt} = -m\gamma\mathbf{v} + \boldsymbol{\xi}(t) \tag{1.20}$$

which is a stochastic equation.

The same consideration can be applied to Brownian motion in the presence of a force field, for example, the gravitational or a harmonic force binding the particle elastically to the origin. If the potential of the force is denoted by V, the equation of motion becomes

$$\begin{aligned} \frac{d\mathbf{p}}{dt} &= -\boldsymbol{\nabla}V - \gamma\mathbf{p} + \boldsymbol{\xi}(t) \\ \frac{d\mathbf{x}}{dt} &= \frac{\mathbf{p}}{m} = \mathbf{v} \end{aligned} \tag{1.21}$$

A set of equations of motion containing a random force, like (1.20) or (1.21), is called a Langevin equation.

The random force $\boldsymbol{\xi}(t)$ is a stochastic process randomly changing in time. Brownian motion $\boldsymbol{v}(t)$ and $\boldsymbol{x}(t)$ are also stochastic processes generated by $\boldsymbol{\xi}(t)$. They are related to $\boldsymbol{\xi}(t)$ by (1.20) *or* (1.21). *If we consider the force causing the motion, then the random force $\boldsymbol{\xi}(t)$ produces Brownian motion. Thus our problem is to determine the stochastic processes $\boldsymbol{v}(t)$ and $\boldsymbol{x}(t)$ from knowing $\boldsymbol{\xi}(t)$. This is what is meant by solving stochastic equations like* (1.20) *or* (1.21).[4]

1.4 Brownian Motion Modeled by a Gaussian Process.

The Langevin equation (1.21) depicts Brownian motion as driven by the random force $\boldsymbol{\xi}(t)$. As an idealization of Brownian motion, $\boldsymbol{\xi}(t)$ is assumed to satisfy the following conditions:

1. $\boldsymbol{\xi}(t)$ is zero mean Gaussian process.

2. $\boldsymbol{\xi}(t)$ has a white spectrum, which means that the values of the random variable in two different instants of time do not keep statistical correlation.

The first condition can be expressed mathematically as follows

$$\langle \boldsymbol{\xi}(t) \rangle = 0, \tag{1.22}$$

for the second condition we define the autocorrelation function of the force $\boldsymbol{\xi}(t)$,

$$g(t') = \langle \boldsymbol{\xi}(t)\boldsymbol{\xi}(t+t') \rangle, \tag{1.23}$$

is an even function of t', decreasing over a characteristic time τ_c (correlation time). The time step considered to solve the equations must be $dt \ll \gamma^{-1}$[5] (it will be proved later). The simulations carried out consider time steps up to 6 orders of magnitude smaller than γ^{-1}.

We set

$$\int_{-\infty}^{+\infty} g(t')dt' = 2\mathcal{D}m^2, \tag{1.24}$$

the meaning of the parameter $\mathcal{D}$ will be made precise later. As we said previously, the values of the random variable will not be correlated for different instants of time, so (1.23) should be

$$\langle \boldsymbol{\xi}(t)\boldsymbol{\xi}(t+t') \rangle = 2\mathcal{D}m^2\boldsymbol{\delta}(t-t'). \tag{1.25}$$

In fact, this assumption seem very plausible if Brownian particles are far larger than the molecules of the surrounding fluid. The force $\boldsymbol{\xi}(t)$ acting on a Brownian particle results from a great many impacts from the fluid molecules, so that the Gaussian property is expected to hold by the central limit theorem. Secondly, the time constant of the motion of fluid molecules will be much shorter than the characteristic time of the Brownian particle if the mass of a Brownian particle is much larger than that of fluid molecules. (Rigorously speaking, this is not quite sufficient. This idealization of $\boldsymbol{\xi}(t)$ is legitimate only in the limit of very large mass density of the Brownian particle.) If that is the case, as an idealization the characteristic time of successive impacts from fluid molecules may be considered as infinitely short.[4]

Chapter 2

Systems in thermal equilibrium.

Abstract

En este capítulo nos centramos en sistemas que se encuentran en contacto con un único baño térmico. Estos sistemas son capaces de alcanzar el equilibrio cuando transcurre el tiempo suficiente, estudiaremos el comportamiento de los valores medios de las diferentes cantidades dinámicas de la partícula en el regimen de transición al equilibrio y una vez alcanzado éste.

También se presenta una alternativa para resolver las ecuaciones de movimiento, el análisis armónico.

This work focuses on the study of reduced dimensionality systems, so from now on we will focus on a single dimension. Although extrapolating the results obtained in this work to higher dimensionalities might be possible, it will not be done here. The one-dimensional version of equation (1.21) is

$$\begin{aligned} \frac{dp}{dt} &= -\frac{\partial V}{\partial x} - \gamma p + \xi(t) \\ \frac{dx}{dt} &= \frac{p}{m} = v. \end{aligned} \tag{2.1}$$

2.1 Free particle.

The simplest case within the systems in contact with a thermal reservoir that reach the equilibrium is that of the free particle. (Figure 2.1)

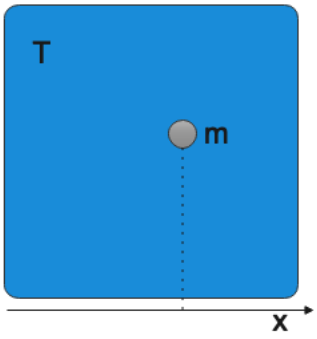

Figure 2.1: Scheme of the system for the case of the free particle with mass m. The colored region denotes the thermal reservoir that is at temperature T.

2.1.1 Evolution of the velocity from a well-defined initial value.

Lets assume that the particle has a well-defined value for his velocity. This value, that is not random, is

$$v(0) = v_0. \tag{2.2}$$

If there is no external force applied the equation (2.1) takes the following form

$$\begin{aligned} \frac{dp}{dt} &= -\gamma p + \xi(t) \\ \frac{dx}{dt} &= \frac{p}{m} = v. \end{aligned} \tag{2.3}$$

The solution of equation (2.3) corresponding to the initial condition (2.2) is given by

$$v(t) = v_0 e^{-\gamma t} + \frac{1}{m}\int_0^t \xi(t')e^{-\gamma(t-t')}dt', \quad t > 0. \tag{2.4}$$

As we saw in Section 1.3, the velocity $v(t)$ of the Brownian particle is a random process generated by the action of $\xi(t)$. Observing equation (2.4) we can see that this process is not stationary. We calculate the average value of $v(t)$ at any time $t > 0$, since we know that the average value of ξ must satisfy (1.22)

$$\langle v(t)\rangle = v_0 e^{-\gamma t}, \quad t > 0. \tag{2.5}$$

The average value of the velocity decays exponentially to zero with a relaxation time constant $\tau_r = \gamma^{-1}$. (Figure 2.2)

The variance of the velocity is defined for instance by the formula

$$\sigma_v^2(t) = \langle [v(t) - \langle v(t)\rangle]^2\rangle. \tag{2.6}$$

From (2.4) and (2.5) we get

$$\sigma_v^2(t) = \frac{1}{m^2}\int_0^t dt' \int_0^t dt'' \langle \xi(t')\xi(t'')\rangle e^{-\gamma(t-t')}e^{-\gamma(t-t'')}. \tag{2.7}$$

When the autocorrelation function of the Langevin force is given by (1.23), we obtain

$$\sigma_v^2(t) = 2\mathcal{D}\int_0^t e^{-2\gamma(t-t')}dt', \tag{2.8}$$

that is

$$\sigma_v^2(t) = \frac{\mathcal{D}}{\gamma}(1 - e^{-2\gamma t}), \quad t > 0. \tag{2.9}$$

At time $t = 0$, the variance of the velocity vanishes (the initial velocity is a non-random variable). Under the effect of the Langevin force, velocity fluctuations arise, and the variance $\sigma_v^2(t)$ increases with time. At first, this increase is linear

$$\sigma_v^2(t) \simeq 2\mathcal{D}t, \quad t \ll \tau_r. \tag{2.10}$$

We can interpret formula (2.10) *as describing a phenomenon of diffusion in the velocity space. The parameter* $\mathcal{D}$*, which has been introduced in* (1.23)*, takes the meaning of a diffusion coefficient in the velocity space.*[6] The variance of the velocity does not however increase indefinitely, but ends up saturating at the value $\mathcal{D}/\gamma$ (Figure 2.2)

$$\sigma_v^2(t) \simeq \frac{\mathcal{D}}{\gamma}, \quad t \gg \tau_r. \tag{2.11}$$

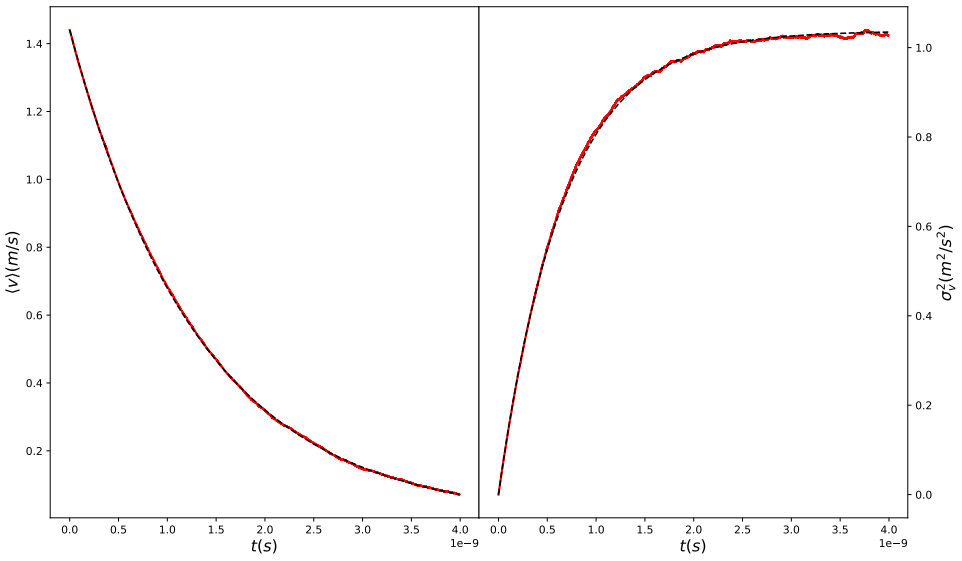

Figure 2.2: Average velocity (left) and variance of velocity (right) of the Brownian particle. The red solid line corresponds to the numerical simulation and the black dotted line to the theoretical results (2.5)(left) and (2.9)(right) for the particular case of $m = 6.65 \times 10^{-26}$ kg, $\gamma = (5 \times 10^{-17})/m\ s^{-1}$, $T = 5 \times 10^{-3}$ K and the statistical average was made over 10^4 stochastic trajectories.

2.1.2 Second fluctuation-dissipation theorem.

Another possible expression for the variance of the velocity is

$$\sigma_v^2(t) = \langle v^2(t) \rangle - \langle v(t) \rangle^2. \tag{2.12}$$

When $t \gg \tau_r$, the average of the velocity tends towards zero (see (2.5)). Taking into account equations (2.11) and (2.12) we see that the value of $\langle v^2(t) \rangle$ tends to the limit value $\mathcal{D}/\gamma$ regardless of the value of v_0. On the other hand, the average energy $\langle E \rangle = m\langle v^2(t) \rangle/2$ tends towards the corresponding limit $\langle E \rangle = m\mathcal{D}/2\gamma$.

If we consider that the bath is in thermodynamic equilibrium with itself at a temperature T, the average energy of the particle in equilibrium which is given by the equipartition theorem will be $\langle E \rangle = k_B T/2$. Comparing both expressions for $\langle E \rangle$, we get a relation between the diffusion coefficient $\mathcal{D}$ in the velocity space, associated with the velocity fluctuations, and the friction coefficient γ, which characterizes the dissipation

$$\boxed{\gamma = \frac{m}{k_B T}\mathcal{D}.} \tag{2.13}$$

Using expression (2.13), we can rewrite equation (1.24) in the form

$$\boxed{\gamma = \frac{1}{2mk_BT}\int_{-\infty}^{+\infty}\langle\xi(t)\xi(t+t')dt',} \tag{2.14}$$

and equation (1.25) can be rewrite as

$$\langle\xi(t)\xi(t+t')\rangle = 2mk_BT\gamma\delta(t-t'). \tag{2.15}$$

Equation (2.14) relates the friction coefficient to the autocorrelation function of the Langevin force. It is known as the *second fluctuation-dissipation theorem.*

In the Langevin equation (2.1)*, the force on a Brownian particle was divided into frictional force* $-m\gamma v$ *and the random force* $\xi(t)$*, between which a relationship like* (2.15) *exist , indicating that the power intensity of* $\xi(t)$ *is proportional to the friction coefficient and the thermal energy* k_BT*. This express that such a mechanism of energy dissipation is closely related to fluctuations in thermal equilibrium and they are simple examples of a more general principle called the fluctuation-dissipation theorem.*[4]

2.1.3 Evolution of the displacement from a well-defined initial position: diffusion of the Brownian particle.

Now we assume in the same way that for the velocity that at the instant $t = 0$ the Brownian particle has a well-defined value for its position

$$x(0) = x_0. \tag{2.16}$$

Integrating equation (2.5) between the instants 0 and t, we obtain by applying the initial condition (2.16) the expression

$$x(t) = x_0 + \frac{v_0}{\gamma}(1-e^{-\gamma t}) + \frac{1}{m}\int_0^t \frac{1-e^{-\gamma(t-t')}}{\gamma}\xi(t')dt', \quad t > 0. \tag{2.17}$$

We see that the displacement of the Brownian particle is also a non-stationary stochastic process like the velocity. Calculating its average value as a function of time we obtain

$$\langle x(t)\rangle = x_0 + \frac{v_0}{\gamma}(1-e^{-\gamma t}), \quad t > 0. \tag{2.18}$$

For very large time values $t \gg \tau_r$ the displacement of the Brownian particle $\langle x(t)\rangle - x_0$ tends to the finite value v_0/γ. (Figure 2.3)

The variance of the displacement $x(t) - x_0$ matches the variance of $x(t)$, defined as

$$\sigma_x^2(t) = \langle[x(t) - \langle x(t)\rangle]^2\rangle. \tag{2.19}$$

Using (2.17) and (2.18), we get

$$\sigma_x^2(t) = \frac{1}{m^2\gamma^2}\int_0^t dt'\int_0^t dt''\langle\xi(t')\xi(t'')\rangle[1-e^{-\gamma(t-t')}][1-e^{-\gamma(t-t'')}], \tag{2.20}$$

taking for the autocorrelation function of $\xi(t)$ the expression (1.25) we have

$$\sigma_x^2(t) = \frac{2\mathcal{D}}{\gamma^2}\int_0^t (1-e^{-\gamma t'})^2 dt'. \tag{2.21}$$

Integrating the previous expression, we obtain

$$\sigma_x^2(t) = \frac{2\mathcal{D}}{\gamma^2}\left(t - 2\frac{1-e^{-\gamma t}}{\gamma} + \frac{1-e^{-2\gamma t}}{2\gamma}\right), \quad t > 0. \tag{2.22}$$

Starting from its vanishing initial value, the variance of the displacement increases, first as $2\mathcal{D}t^3/3$ for $t \ll \tau_r$, then as $2\mathcal{D}t/\gamma^2$ for $t \gg \tau_r$. (Figure 2.3)

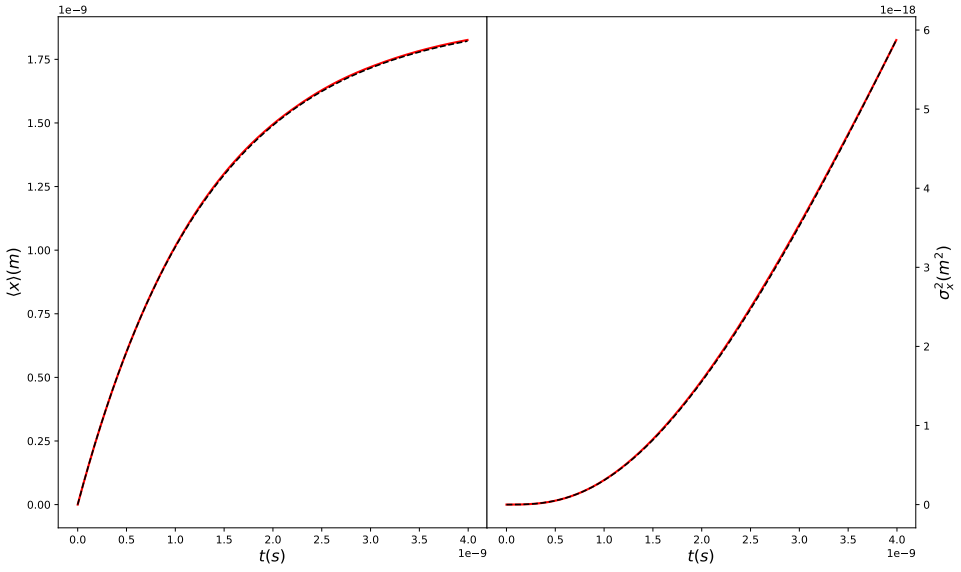

Figure 2.3: Average position (left) and variance of position (right) of the Brownian particle. The red solid line corresponds to the numerical simulation and the black dotted line to the theoretical results (2.5)(left) and (2.9)(right) for the particular case of $m = 6.65 \times 10^{-26}$ kg, $\gamma = (5 \times 10^{-17})/m\ s^{-1}$, $T = 5 \times 10^{-3}$ K and the statistical average was made over 10^4 stochastic trajectories.

On the other hand, since $x(t) - x_0 = x(t) + \langle x(t)\rangle - \langle x(t)\rangle - x_0$, we have

$$\langle [x(t) - x_0]^2\rangle = \sigma_x^2(t) + \frac{v_0^2}{\gamma^2}(1-e^{-\gamma t})^2, \quad t > 0. \tag{2.23}$$

For $t \gg \tau_r$, we therefore obtain

$$\langle [x(t) - x_0]^2\rangle \simeq 2\frac{\mathcal{D}}{\gamma^2}t. \tag{2.24}$$

Observing (2.22) *and* (2.24) *we see that the Brownian particle diffuses at large times. We also see that the diffusion coefficient D is related with the diffusion coefficient in the velocity space $\mathcal{D}$ by the formula* [6]

$$\boxed{D = \frac{\mathcal{D}}{\gamma^2}.} \tag{2.25}$$

2.1.4 Thermal equilibrium.

A system in contact with a single thermal reservoir tends to a state of equilibrium in which it is at the same temperature as said reservoir. We should wait for our Brownian particle to reach its bath temperature T after enough time has elapsed. We can check this by calculating the temperature of the particle using definition (A.11) and the velocity obtained from the simulation. (Figure 2.4)

But how can we know that equilibrium has been reached? When the particle reaches equilibrium, we know that its velocity distribution must be the Maxwell-Boltzmann distribution, or in other words, the velocity component must present a Gaussian-type distribution with zero mean.

A standard criteria to measure the deviation of a symmetric distribution from Gaussian is thus the kurtosis ($\mathcal{K}$)

$$\mathcal{K} = \frac{\langle(\nu - \langle\nu\rangle)^4\rangle}{\langle(\nu - \langle\nu\rangle)^2\rangle^2} - 3. \tag{2.26}$$

Comparing to Gaussian distribution, zero $\mathcal{K}$ indicates that it is a Gaussian distribution, a positive $\mathcal{K}$ implies a narrower central peak and two fatter tails; and vice versa.[3]

Figure 2.4 shows the temporal evolution of the particle's kinetic temperature and the kurtosis values associated with its velocity distribution.

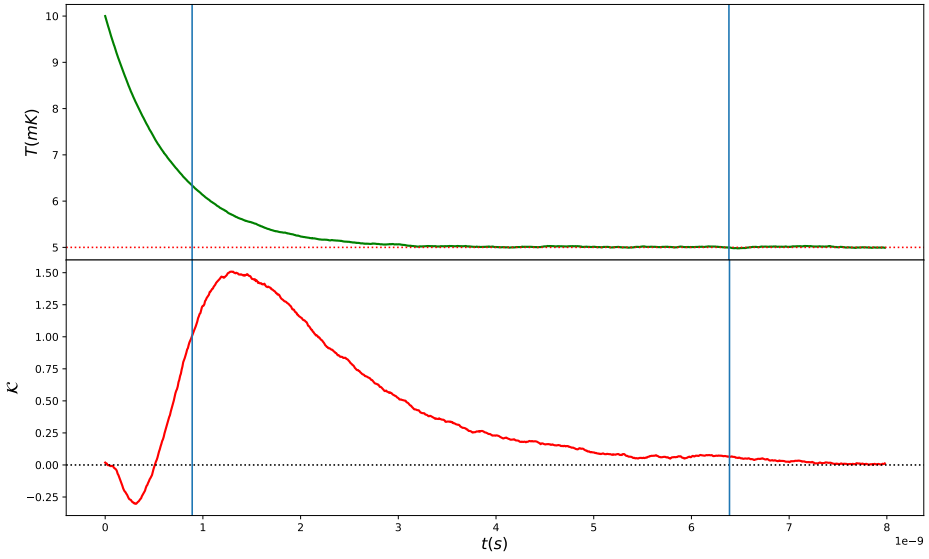

Figure 2.4: Kinetic temperature (top) and kurtosis of the velocity distribution (bottom) of a Brownian particle. The blue lines represent the instants in which the velocity distributions are taken for figure 2.5. The particle starts from a velocity that corresponds to a temperature 2 times higher than that of the bath for the particular case of $m = 6.65 \times 10^{-26}$ kg, $\gamma = (5 \times 10^{-17})/m\ s^{-1}$, $T = 5 \times 10^{-3}$ K and the statistical average was made over 10^5 trajectories.

The zero decay of kurtosis is observed as the kinetic temperature approaches the bath temperature. Which would correspond to the situation of thermal equilibrium. Below we show the velocity distributions at the instants indicated by the blue lines in figure 2.4.

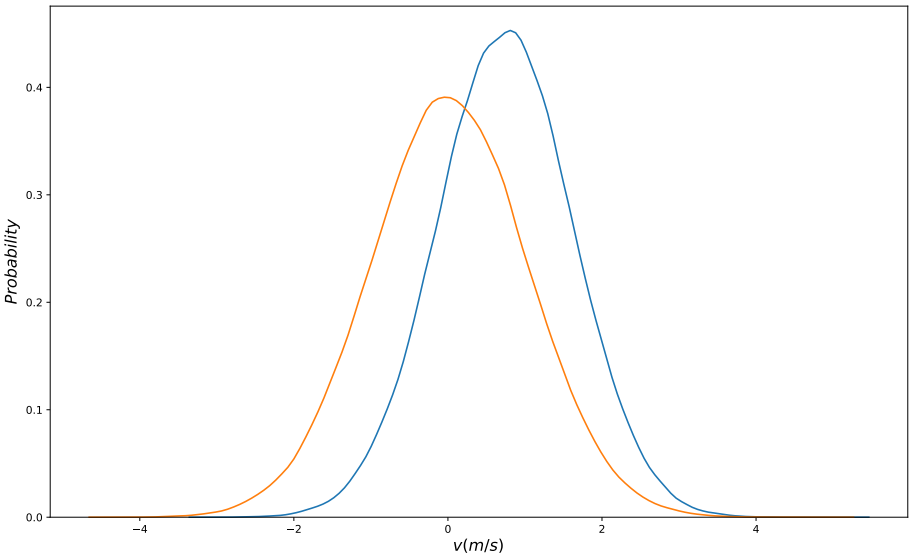

Figure 2.5: The blue distribution corresponds to the blue line on the left (non-equilibrium) in figure 2.4 while the orange one corresponds to the one on the right (equilibrium).

2.1.5 Equilibrium velocity fluctuations.

We are interested here in the dynamics of the velocity fluctuations of a Brownian particle in equilibrium with the bath. We assume, as previously, that the latter is in thermodynamic equilibrium at temperature T.

To obtain the expression for the velocity of the Brownian particle at equilibrium, we first write the solution $v(t)$ of the Langevin equation for the initial condition $v(t_0) = v_0$

$$v(t) = v_0 e^{-\gamma(t-t_0)} + \frac{1}{m}\int_{t_0}^{t} \xi(t')e^{-\gamma(t-t')}dt'. \tag{2.27}$$

We then take the limit $t_0 \to -\infty$. As shown by the formula (2.27), the initial value of the velocity is "forgotten" and $v(t)$ reads

$$v(t) = \frac{1}{m}\int_{-\infty}^{t} \xi(t')e^{-\gamma(t-t')}dt'. \tag{2.28}$$

In these conditions, at any finite time t, the particle is in equilibrium with the bath. Its velocity $v(t)$ is a stationary random process. Since the average value of the velocity vanishes at equilibrium, the autocorrelation function of $v(t)$, which we will now compute, represents the dynamics of the equilibrium velocity fluctuations.[6]

Correlation function between the Langevin force and the velocity.

Starting from (2.28), it is possible to compute the correlation function $\langle v(t)\xi(t')\rangle$

$$\langle v(t)\xi(t')\rangle = \frac{1}{m}\int_{-\infty}^{t} \langle \xi(t'')\xi(t')\rangle e^{-\gamma(t-t'')}dt''. \tag{2.29}$$

When the autocorrelation function of the Langevin force is of the form (1.25), equation (2.29) reads

$$\langle v(t)\xi(t')\rangle = 2\mathcal{D}m\int_{-\infty}^{t}\delta(t'-t'')e^{-\gamma(t-t'')}dt''. \tag{2.30}$$

From formula (2.30), we get

$$\langle v(t)\xi(t')\rangle = \begin{cases} 2\mathcal{D}me^{-\gamma(t-t')}, & t' < t \\ 0, & t' > t. \end{cases} \tag{2.31}$$

This expression display the fact that the Brownian particle velocity at time t is not correlated with the Langevin force at a subsequent time $t' > t$ which is in accordance with classical causality.

Equilibrium velocity autocorrelation function.

When the velocity $v(t)$ is given by expression (2.28), the autocorrelation function $\langle v(t)v(t')\rangle$ will be

$$\langle v(t)v(t')\rangle = \frac{1}{m}\int_{-\infty}^{t}\langle \xi(t''v(t'))\rangle e^{-\gamma(t-t'')}dt''. \tag{2.32}$$

Taking the equation (2.31) into account, we get

$$\langle v(t)v(t')\rangle = \frac{\mathcal{D}}{\gamma}e^{-\gamma|t-t'|} \tag{2.33}$$

or setting $t' = 0$

$$\boxed{\langle v(t)v(t')\rangle = \frac{\mathcal{D}}{\gamma}e^{-\gamma|t|}}. \tag{2.34}$$

The decrease of the velocity autocorrelation function is described by an exponential of time constant $\tau_r = \gamma^{-1}$. (Figure 2.6)

We observe that the time in which the velocity correlation decays to zero coincides with that in which the kurtosis falls to zero, at least to a good first approximation.

2.2 Particle confined by a harmonic potential.

Now we will suppose that an harmonic force acts on our Brownian particle that keeps its motion confined to a certain region of space. (Figure 2.7)

Langevin's equation (2.1) in this case takes the form

$$\begin{aligned} \frac{dp}{dt} &= -mw_0^2x - \gamma p + \xi(t) \\ \frac{dx}{dt} &= \frac{p}{m} = v, \end{aligned} \tag{2.35}$$

where w_0 is the frequency associated with the harmonic force.

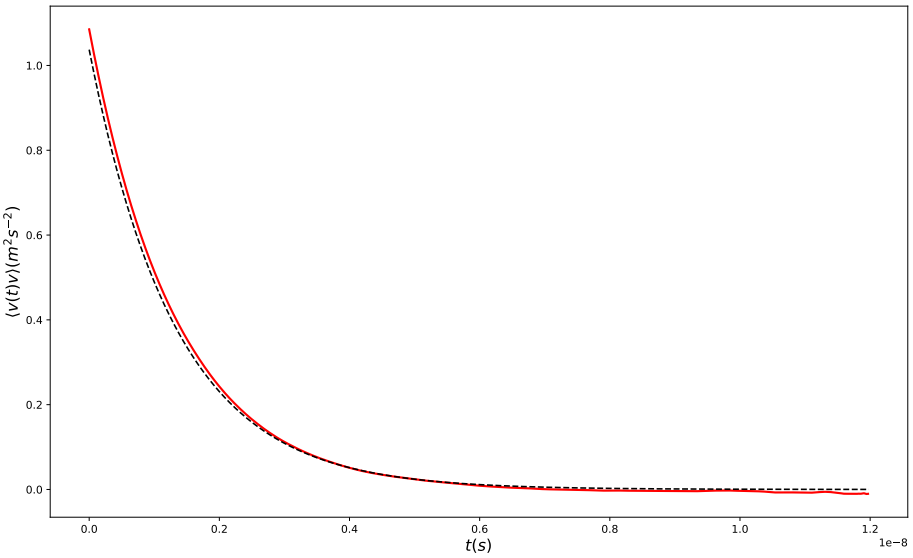

Figure 2.6: Velocity autocorrelation function of the Brownian particle. The red solid line corresponds to the numerical simulation and the black dotted line to the theoretical result (2.34) for the particular case of $m = 6.65 \times 10^{-26}$ kg, $\gamma = (5 \times 10^{-17})/m\ s^{-1}$, $T = 5 \times 10^{-3}$ K and the statistical average was made over 10^4 stochastic trajectories.

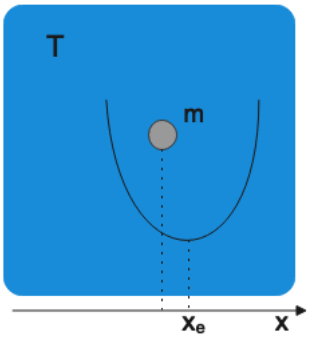

Figure 2.7: Scheme of a particle confined by a harmonic potential. The colored region denotes the thermal deposit at a temperature of T.

2.2.1 Position, velocity and temperature.

Writing equation (2.35) completely in terms of position

$$\frac{d^2x}{dt^2} + \frac{\gamma}{m}\frac{dx}{dt} + w_0^2 x = \frac{1}{m}\xi(t). \tag{2.36}$$

Making mean values on both sides of the expression and considering the condition (2.22), we get

$$\frac{d^2\langle x\rangle}{dt^2} + \frac{\gamma}{m}\frac{d\langle x\rangle}{dt} + w_0^2\langle x\rangle = 0. \tag{2.37}$$

Equation (2.37) is a second order homogeneous equation whose initial conditions are (2.16) and (2.2) respectively since we consider that the Brownian particle starts from well-defined values for both its position and its velocity. These types of equations have known solutions due to their wide use in different frameworks of physics and mathematics, it is not the concern

of this work to stop to comment on these methods, therefore, we are going directly to see the solutions that we have obtained after its resolution. (Figure 2.8)

According to what values the parameters take, the solutions adopt two different behaviors

- Periodic behavior ($w_0 > \gamma/2m$).

$$\langle x(t)\rangle_p = \frac{e^{-\frac{\gamma}{2m}t}}{w_1}\left[\left(v_0 + \frac{\gamma}{2m}x_0\right)\sin(w_1 t) + w_1 x_0 \cos(w_1 t)\right], \tag{2.38}$$

  where w_1 is given by $\sqrt{w_0^2 - \gamma^2/4m^2}$. The values of x_0 and v_0 are given by (2.16) and (2.2).

- Damped behavior ($w_0 < \gamma/2m$).

$$\langle x(t)\rangle_d = \frac{e^{-\frac{\gamma}{2m}t}}{w_1}\left[\left(v_0 + \frac{\gamma}{2m}x_0\right)\sinh(w_1 t) + w_1 x_0 \cosh(w_1 t)\right], \tag{2.39}$$

  and in this case w_1 is of the form $\sqrt{\gamma^2/4m^2 - w_0^2}$.

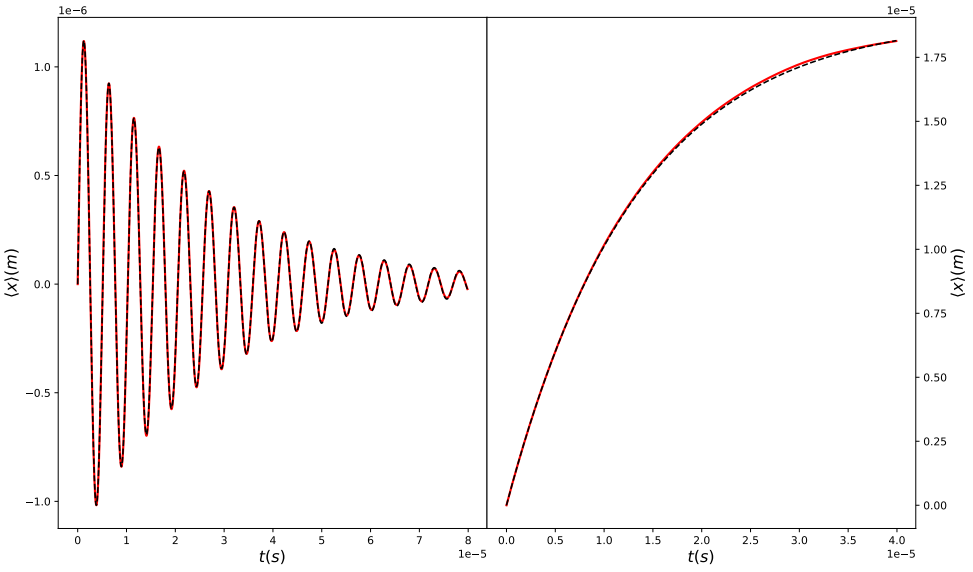

Figure 2.8: Average position of the Brownian particle into a harmonic potential. The red solid line corresponds to the numerical simulation and the black dotted line to the theoretical periodic (2.38) and damped (2.39) results for the particular case of $m = 6.65\times10^{-26}$ kg, $\gamma = (5\times 10^{-21})/m\ s^{-1}$, $T = 5\times10^{-3}$ K, the statistical average was made over 10^4 stochastic trajectories, $w_0^2 = 10^{-13}/ms^{-1}$ on the left (periodic) and $w_0^2 = 10^{-18}/ms^{-1}$ on the right (damped).

In the periodic case, the average value of the position tends to the value where the minimum of the potential is found, while the function decays it behaves like a combination of sinusoidal

functions. On the other hand, for the damped case it grows as a combination of hyperbolic functions.

Derivating equations (2.38) and (2.39) with respect to time, the corresponding expressions for velocity are obtained (Figure 2.9)

- Periodic behavior ($w_0 > \gamma/2m$).

$$\begin{aligned}\langle v(t)\rangle_p = e^{-\frac{\gamma}{2m}t}\Big\{&\Big[\Big(v_0+\frac{\gamma}{2m}x_0\Big)\cos(w_1t) - w_1x_0\sin(w_1t)\Big]\\ &-\frac{\gamma}{2mw_1}\Big[\Big(v_0+\frac{\gamma}{2m}x_0\Big)\sin(w_1t)+w_1x_0\cos(w_1t)\Big]\end{aligned} \tag{2.40}$$

- Damped behavior ($w_0 < \gamma/2m$).

$$\begin{aligned}\langle v(t)\rangle_d = e^{-\frac{\gamma}{2m}t}\Big\{&\Big[\Big(v_0+\frac{\gamma}{2m}x_0\Big)\cosh(w_1t) + w_1x_0\sinh(w_1t)\Big]\\ &-\frac{\gamma}{2mw_1}\Big[\Big(v_0+\frac{\gamma}{2m}x_0\Big)\sinh(w_1t)+w_1x_0\cosh(w_1t)\Big]\end{aligned} \tag{2.41}$$

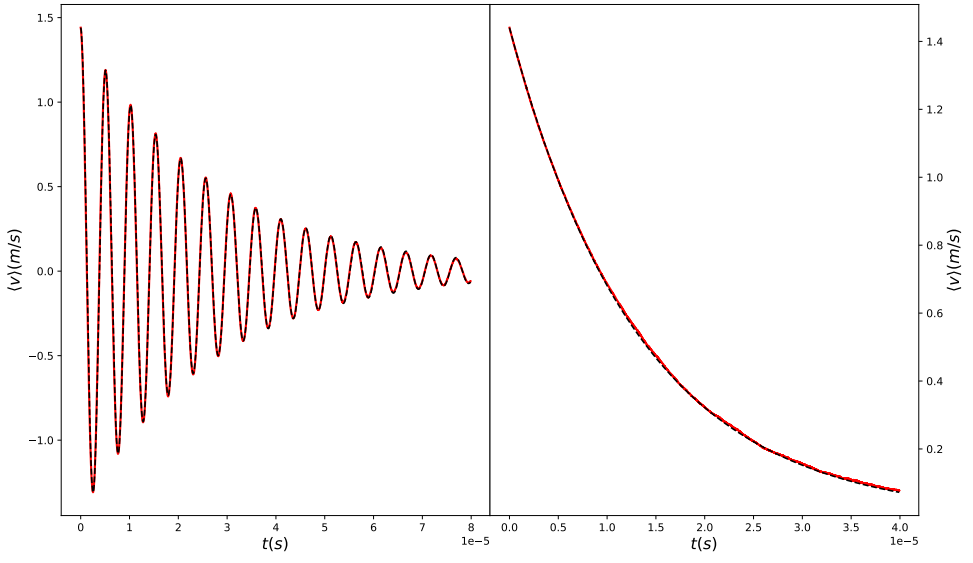

Figure 2.9: Average velocity of the Brownian particle into a harmonic potential. The red solid line corresponds to the numerical simulation and the black dotted line to the theoretical periodic (2.40) and damped (2.41) results for the particular case of $m = 6.65\times10^{-26}$ kg, $\gamma = (5\times 10^{-21})/m\ s^{-1}$, $T = 5\times10^{-3}$ K, the statistical average was made over 10^4 stochastic trajectories, $w_0^2 = 10^{-13}/ms^{-1}$ on the left (periodic) and $w_0^2 = 10^{-18}/ms^{-1}$ on the right (damped).

For the temperature we proceed in the same way as in Section 2.1.4. Obtaining that, as in the case of the free particle, it thermalizes to bath temperature after sufficient time elapses.

But while in the damped case we recover a kurtosis profile very similar to that of the free particle case (as expected), we observe that for the periodic case a profile modulated by the same pattern appears but it presents a series of oscillations with minimum values very close to zero. (Figure 2.10)

As shown for the case of the free particle, a zero decay of the kurtosis is observed as the kinetic temperature approaches that of the bath. Which corresponds to the situation of thermal equilibrium.

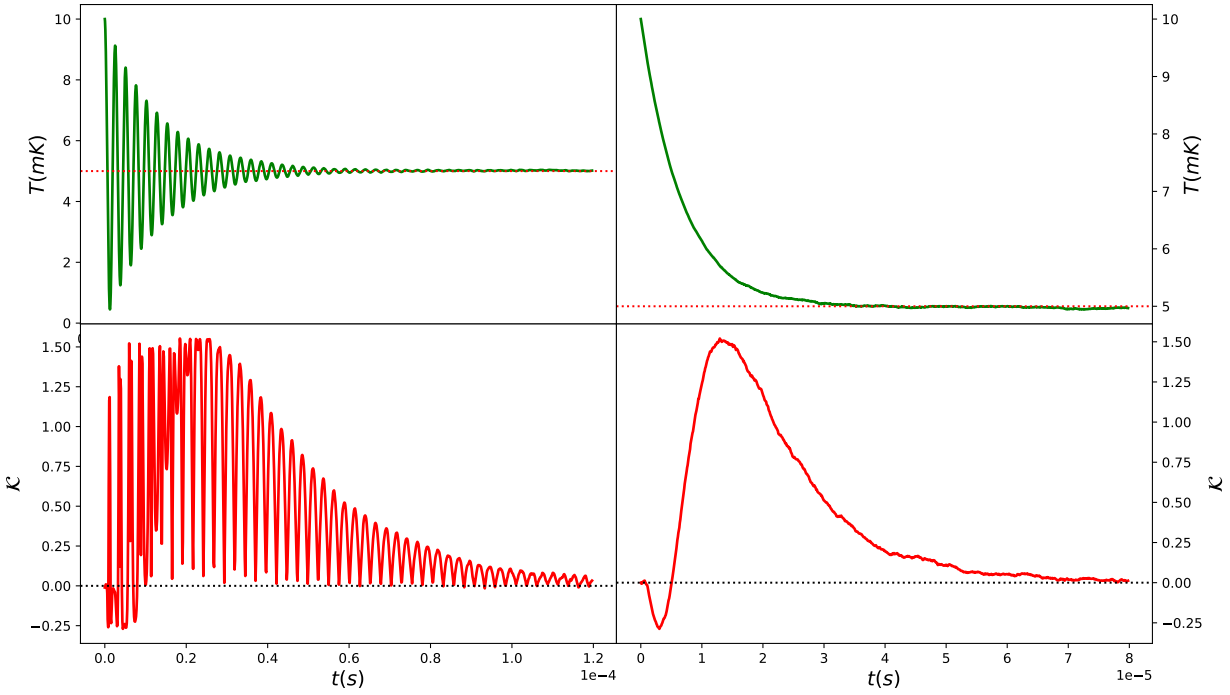

Figure 2.10: Kinetic temperature (top) and kurtosis of the velocity distribution (bottom) of a Brownian particle into a harmonic potential. The particle starts from a velocity that corresponds to a temperature 2 times higher than that of the bath for the particular case of $m = 6.65 \times 10^{-26}$ kg, $\gamma = (5 \times 10^{-21})/m\ s^{-1}$, $T = 5 \times 10^{-3} K$, the statistical average was made over 10^5 stochastic trajectories, $w_0^2 = 10^{-13}/ms^{-1}$ on the left (periodic) and $w_0^2 = 10^{-18}/ms^{-1}$ on the right (damped).

2.2.2 Harmonic analysis of the Langevin model.

Let $Y(t)$ be a stationary stochastic process. The harmonic analysis of this process consists in studying the properties of the Fourier series of $Y(t)$, or those of its Fourier transform.

It has however to be carried out with some caution, since any given realization $y(t)$ of the process is, a priori, neither a periodic function expandable in Fourier series, nor function integrable or square-integrable possesing a well-defined Fourier transform.[6]

Fourier transform of a stationary process.

A realization $y(t)$ of the stationary process $Y(t)$ does not vanish as $t \to \pm\infty$. The function $y(t)$ is thus neither integrable nor square-integrable, and its Fourier transform does not exist in the ordinary sense. We can however define width $\mathcal{T}$ of the time axis. The process under consideration being stationary, this time interval may be taken starting from any origin. We generally, choose the origin $t = 0$. We define the Fourier transform $y(w)$ of the function $y_{\mathcal{T}}(t)$, equal to $y(t)$ over the interval $(0, \mathcal{T})$ and vanishing outside this interval[6]

$$y(w) = \int_{-\infty}^{\infty} y_{\mathcal{T}}(t) e^{iwt} dt = \int_{0}^{\mathcal{T}} y(t) e^{iwt} dt. \tag{2.42}$$

As for the stochastic process $Y(t)$ it self, we sometimes write symbolically (it then being understood that the above described procedure has been used),

$$Y(w) = \int_{-\infty}^{\infty} Y(t) e^{iwt} dt, \tag{2.43}$$

Fourier series of an stationary process.

A realization $y(t)$ of the stationary process $Y(t)$ is not a periodic function. We can nevertheless define its Fourier series. To this end, we consider this function over a large interval of finite width $\mathcal{T}$ of the time axis, taken starting from any origin (we can choose, as previously, the origin $t = 0$). For fixed $\mathcal{T}$, it is possible to expand in Fourier series the function obtained by periodizing $y(t)$. This expansion coincides with $y(t)$ over the interval $0 \leq t \leq \mathcal{T}$ [6]

$$y(t) = \sum_{n=-\infty}^{\infty} a_n e^{-iwt}, \quad 0 \leq t \leq \mathcal{T}. \tag{2.44}$$

The angular frequencies w_n and the Fourier coefficients a_n are given by the usual formulas

$$w_n = \frac{2\pi n}{\mathcal{T}}, \quad a_n = \frac{1}{\mathcal{T}} \int_0^{\mathcal{T}} y(t) e^{iw_n t} dt, \quad n = 0, \pm 1, \pm 2, ... \tag{2.45}$$

The limit $\mathcal{T} \to \infty$ will be taken at the end of the calculation.
As for the (stationary) stochastic process, we write, in a symbolic way

$$Y(t) = \sum_{n=-\infty}^{\infty} A_n e^{-iw_n t}, \quad 0 \leq t \leq \mathcal{T}. \tag{2.46}$$

The Fourier coefficient a_n is a realization of the random variable A_n defined by

$$A_n = \frac{1}{\mathcal{T}} \int_0^{\mathcal{T}} Y(t) e^{iw_n t} dt. \tag{2.47}$$

The value of $\mathcal{T}$ being fixed, we have the relation

$$A_n = \frac{1}{\mathcal{T}} Y(w_n) \tag{2.48}$$

between the Fourier coefficient A_n and the Fourier transform $Y(w_n)$.

Consequences of the stationarity.

Let us now examine the consequences of the stationarity on the coefficients of the Fourier series expansion.

- One-time averages.

The process under consideration being stationary, $\langle Y(t)\rangle = \langle Y\rangle$ is a constant. The average of A_n being given by

$$\langle A_n\rangle = \frac{1}{\mathcal{T}}\int_0^{\mathcal{T}} \langle Y(t)\rangle e^{iw_n t}dt, \tag{2.49}$$

we have:

$$\begin{aligned} &\langle A_n\rangle = 0, \quad n \neq 0 \\ &\langle A_0\rangle = \frac{1}{\mathcal{T}}\int_0^{\mathcal{T}} \langle Y(t)\rangle dt = \langle Y\rangle. \end{aligned} \tag{2.50}$$

A realization a_0 of A_0 is the temporal average of a realization $y(t)$ of the process $Y(t)$ over the interval $(0, \mathcal{T})$

$$a_0 = \overline{y(t)}^{\mathcal{T}} = \frac{1}{\mathcal{T}}\int_0^{\mathcal{T}} y(t)dt. \tag{2.51}$$

All realizations a_0 of A_0 being then equal to $\langle Y\rangle$, A_0 is a non-random variable. We can therefore focus the interest on the centered process $Y(t) - \langle Y\rangle$ and assume, without loss of generality, that we have

$$A_n = 0, \quad n = 0, \pm 1, \pm 2... \tag{2.52}$$

- Two-time averages.

For a stationary process, the two-time averages only depend on the difference of the two times involved. The autocorrelation function $g(\tau) = \langle Y^*(t)Y(t+\tau)\rangle$ of the process $Y(t)$, assumed to be centered, may be written, using the series expansion (2.46), as

$$g(\tau) = \sum_{n=-\infty}^{\infty}\sum_{n'=-\infty}^{\infty} \langle A_n A_{n'}^*\rangle e^{-i(w_n - w_{n'})t} e^{-iw_n\tau}. \tag{2.53}$$

This function having to be independent of t for any τ, we get

$$\langle A_n A_{n'}^*\rangle = \langle |A_n|^2\rangle \delta_{n,n'}. \tag{2.54}$$

Thus, there is no correlation between two Fourier coefficients of unequal angular frequencies.

Spectral density of a stationary centered process.

Let us consider a centered stationary stochastic process $Y(t)$ characterized by real realizations $y(t)$. The Fourier coefficients of $y(t)$ take the form

$$a_n = a'_n + ia''_n, \quad a_{-n} = a^*_n = a'_n - ia''_n. \tag{2.55}$$

The mean square of the Fourier component A_n of $Y(t)$ is

$$\langle |A_n|^2 \rangle = \langle A'^2_n \rangle + \langle A''^2_n \rangle, \tag{2.56}$$

where A'_n and A''_n denote the random variables of respective realizations a'_n and a''_n.

When a convenient filter is used to select the angular frequencies belonging to the interval $(w, w + \Delta w)$, the mean observable intensity is

$$\sigma(w)\Delta w = \sum_{w_n \ in \ (w, w+\Delta w)} \langle |A_n|^2 \rangle. \tag{2.57}$$

The right-hand side of equation (2.57) involves a sum over all angular frequencies included in the considered band of width Δw. The number of modes of this type is

$$\frac{\Delta w}{2\pi/\mathcal{T}} = \frac{\mathcal{T}}{2\pi}\Delta w. \tag{2.58}$$

In the limit $\mathcal{T} \to \infty$, we can write, provided that $\langle |A_n|^2 \rangle$ is a continuous function of the angular frequency

$$\sigma(w) = \lim_{\mathcal{T}\to\infty} \frac{\mathcal{T}}{2\pi} \langle |A_n|^2 \rangle. \tag{2.59}$$

Rather than $\sigma(w)$, we generally use the quantity

$$S(w) = 2\pi\sigma(w) = \lim_{\mathcal{T}\to\infty} \mathcal{T} \langle |A_n|^2 \rangle, \tag{2.60}$$

called the spectral density or the noise spectrum of the process $Y(t)$. Using the relation (2.48), we can also express $S(w)$ as a function of the squared modulus of the Fourier transform $Y(w)$

$$S(w) = \lim_{\mathcal{T}\to\infty} \frac{1}{\mathcal{T}} \langle |Y(w)|^2 \rangle. \tag{2.61}$$

The introduction of the spectral density allows us to make a explicit the continuous limit of equation (2.54) displaying the fact that there is no correlation between Fourier coefficients of unequal angular frequencies. Indeed, in this limit

$$\langle Y(w) Y^*(w') \rangle = 2\pi\delta(w - w')S(w). \tag{2.62}$$

Formula (2.62) has been established assuming that $S(w)$ is a continuous function of w. This relation may also be viewed as defining the spectral density.

The Wiener-Khintchine theorem.

Let us come back to the expression (2.53) for the autocorrelation function, assumed to be integrable, of a center stationary process ergodic in the mean. On account of the decorrelation property (2.56), we have

$$g(\tau) = \sum_{n=-\infty}^{\infty} \langle |A_n|^2 \rangle e^{-iw_n\tau}. \tag{2.63}$$

In the limit $\mathcal{T} \to \infty$, the discrete summation in formula (2.63) is replaced by an integration and we can write, the relation (2.48) being taken into account

$$g(\tau) = \lim_{\mathcal{T}\to\infty} \frac{1}{2\pi\mathcal{T}} \int_{-\infty}^{\infty} \langle |Y(w)|^2 \rangle e^{-iw\tau} dw. \tag{2.64}$$

The autocorrelation function $g(\tau)$ thus appears as the Fourier transform of the spectral density $S(w)$ [6]

$$g(\tau) = \frac{1}{2\pi} \int_{-\infty}^{\infty} S(w) e^{-iw\tau} dw. \tag{2.65}$$

Equation (2.65) *(and the corresponding one for its inverse Fourier transform) constitutes the Wiener-Khintchine theorem, which states that the autocorrelation function and the spectral density of a stationary process form a Fourier transform pair. Both quantities contain the same information on the stochastic process under consideration.*[6]

2.2.3 Equilibrium correlation and cross-correlation functions.

Using this method that we just introduced in the previous section, we will study equilibrium fluctuations for the system we are dealing with.

We omit the mathematical developments to go directly to show the results obtained for the different correlations between variables (Figure 2.11).

The analytical expressions for the harmonic particle autocorrelation and cross-correlation functions have the following form

$$\langle x(0)x(t)\rangle = \frac{k_B T}{m w_0^2} e^{-\frac{\gamma}{2m}t} \left[\cos(w_1 t) + \frac{\gamma}{2m w_1}\sin(w_1 t)\right], \tag{2.66}$$

$$\langle v(0)v(t)\rangle = \frac{k_B T}{m} e^{-\frac{\gamma}{2m}t} \left[\cos(w_1 t) - \frac{\gamma}{2m w_1}\sin(w_1 t)\right], \tag{2.67}$$

$$\langle v(0)x(t)\rangle = -\frac{k_B T}{m w_1} e^{-\frac{\gamma}{2m}t} \sin(w_1 t), \tag{2.68}$$

we have omitted the correlation of the position with the velocity at a later point in time because, it is the same function but with the opposite sign to (2.68), so it does not provide us with more information.

It can be seen that the correlations given by (2.46),(2.47) and (2.48) are combinations of sinusoidal functions that decay exponentially with a time constant $\tau_r = (\gamma/2m)^{-1}$.

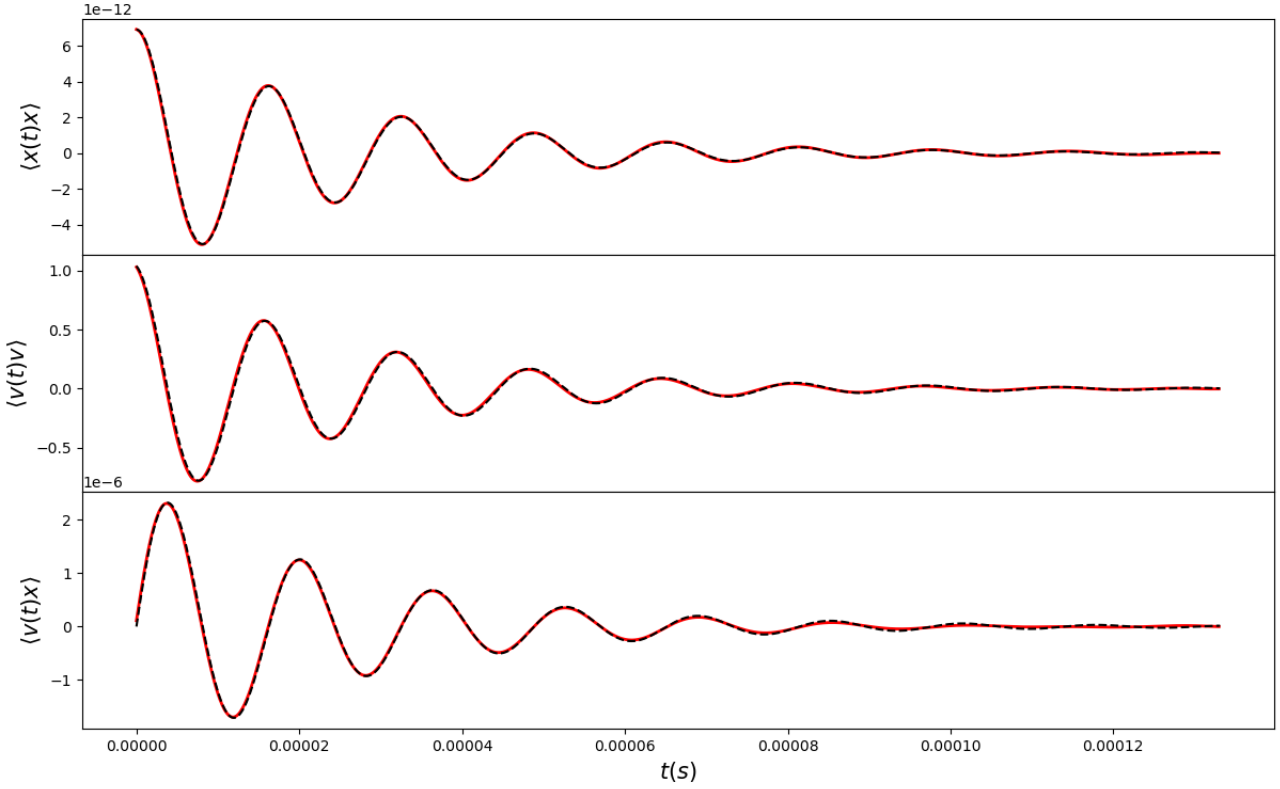

Figure 2.11: Position and velocity correlation functions for the case of harmonic potential. The red solid line corresponds to the numerical simulation and the black dotted line to the theoretical results (2.66),(2.67) and (2.68) for the particular case of $m = 6.65 \times 10^{-26}$ kg, $\gamma = (5 \times 10^{-17})/m\ s^{-1}$, $T = 5 \times 10^{-3}$ K and $w_0^2 = 10^{-14}/ms^{-1}$ (periodic). The stochastic average was made over 10^5 trajectories.

Chapter 3

Systems out of thermal equilibrium.

Abstract

El contenido de este capítulo se centra en estudiar sistemas que son sistemas en los que la acción combinada de distintos baños térmicos determina que el estado estacionario sea de no equilibrio. Caracterizamos dichos estados en términos de la curtosis e introducimos con esto el concepto de equilibrio térmico local (LTE).

Aunque para este tipo de sistemas se vuelve casi imposible obtener soluciones analíticas mostramos un método semi-analítico que nos permite analizar el estado del sistema una vez se encuentre en el estado estacionario estacionario de no equilibrio.

We move on to the study of systems in contact with several baths, for this we focus on the simplest system of this type.(Figure 3.1)

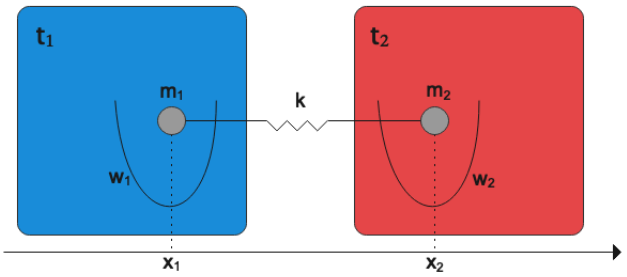

Figure 3.1: Scheme of two particles confined by harmonic potentials and with a harmonic interaction between them. Each particle is in contact with an independent thermal reservoir (colored regions) of temperatures τ_1 and τ_2.

The fact that each particle is in direct contact with a single bath but feels the influence of its neighbor due to the interaction with the other particle causes that, once enough time has elapsed, its temperature stabilizes at an intermediate value between τ_1 and τ_2. Once this stationary state is reached out of equilibrium, the difference between temperatures causes the appearance of heat currents within the system.

3.1 Evolution of a system of two interacting particles.

Through simulations, as in previous cases, we can obtain the temporal evolution of the mean values of velocity and kinetic temperature of both particles. (Figure 3.2)

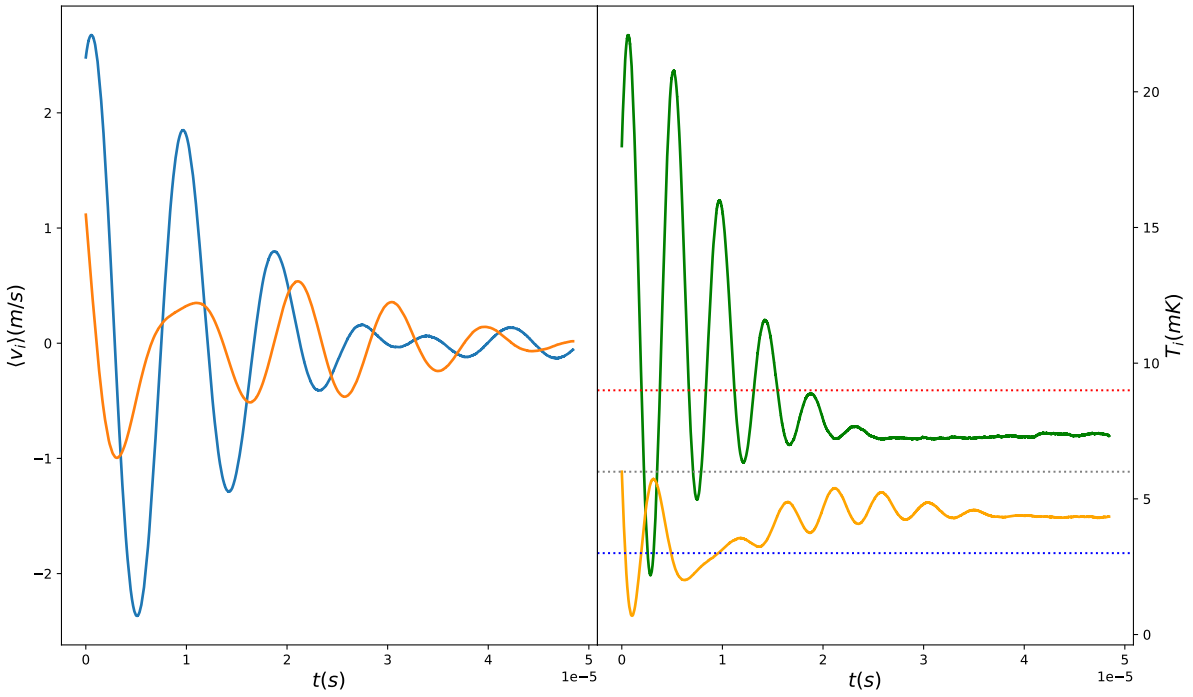

Figure 3.2: On the left, average velocity of particle 1 (blue line) and 2 (orange line). On the right, kinetic temperature of particle 1 (green line) and 2 (yellow line), the dotted lines represent the temperatures of baths 1 (red), 2 (blue) and the average of both (black). The results were obtained for the case of $m_1 = 6.65 \times 10^{-26}(kg)$, $m_2 = 4.03 \times 10^{-26}(kg)$, $\tau_1 = 9mK$, $\tau_2 = 3mK$, $\gamma_1 = 5 \times 10^{-21} kg/s$, $\gamma_2 = 1 \times 10^{-20} kg/s$, $k = 1 \times 10^{-14} kg/s^2$, $w_1^2 = 2k/m_1 s^{-1}$, $w_2^2 = 3k/m_2 s^{-1}$ and with both particles having a kinetic temperature 2 times higher than their corresponding bath temperature.

Both particles reach a steady state out of equilibrium in which they have an intermediate temperature between that of both thermal baths. On the other hand, we see that the mean value of the velocity falls to zero for both particles in the same way as in the systems that reached thermal equilibrium. As we said in the introduction to this chapter, the temperature difference in the final steady state causes heat currents to appear in the system. But how can we characterize them?

The Hamiltonian of the two particles has the form

$$H_s = \frac{p_1^2}{2m_1} + \frac{p_2^2}{2m_2} + V_1(x_1) + V_2(x_2) + V_{int}(x_1, x_2) \tag{3.1}$$

where V_1 and V_2 are the harmonic potentials that act on each particle, while V_{int} is the interaction potential between the two.

The time derivative of this Hamiltonian

$$\frac{dH_s}{dt} = \frac{p_1}{m_1}\frac{dp_1}{dt} + \frac{p_2}{m_2}\frac{dp_2}{dt} + \frac{dV_1}{dx_1}\frac{dx_1}{dt} + \frac{dV_2}{dx_2}\frac{dx_2}{dt} + \frac{\partial V_{int}}{\partial x_1}\frac{dx_1}{dt} + \frac{\partial V_{int}}{\partial x_2}\frac{dx_2}{dt}. \tag{3.2}$$

Considering the Langevin equations for this system

$$\begin{aligned} \frac{dx_1}{dt} &= \frac{p_1}{m_1}; & \frac{dx_2}{dt} &= \frac{p_2}{m_1} \\ \frac{dp_1}{dt} &= -\frac{dV_1}{dx_1} - \frac{\partial V_{int}}{\partial x_1} - \gamma_1 p_1 + \xi_1(t); & \frac{dp_2}{dt} &= -\frac{dV_2}{dx_2} - \frac{\partial V_{int}}{\partial x_2} - \gamma_2 p_2 + \xi_2(t), \end{aligned} \tag{3.3}$$

using the relations expressed in (3.3) we can rewrite (3.2) and then simplify to get

$$\frac{dH_s}{dt} = \frac{p_1}{m_1}\left(-\gamma_1 p_1 + \xi_1(t)\right) + \frac{p_2}{m_2}\left(-\gamma_2 p_2 + \xi_2(t)\right). \tag{3.4}$$

The temporal variation of the total energy of the two particles is given by the sum of all the heat currents of the particles with their respective baths, therefore

$$\frac{d\langle H_s\rangle}{dt} = j_1 + j_2, \tag{3.5}$$

where j_i refers to the heat flow between the particle i and the bath i.

Taking mean values in equation (3.4) and identifying terms we arrive at an expression for the heat currents

$$j_i = -\gamma_i \left\langle \frac{p_i^2}{m_i} \right\rangle + \left\langle \frac{p_i}{m_i}\xi_i(t) \right\rangle, \tag{3.6}$$

how can we calculate the second term of (3.6) if it involves a function that does not have an analytical form, such as $\xi_i(t)$? For this we will use a mathematical result known as Novikov's Theorem that we introduce below.

Novikov theorem.

Novikov theorem states that for a multivariate Gaussian distribution with zero mean

$$P(\boldsymbol{x}) = \sqrt{\frac{det\hat{A}}{(2\pi)^n}} exp\left(-\frac{1}{2}\boldsymbol{x}\cdot\hat{A}\cdot\boldsymbol{x}\right), \tag{3.7}$$

the averages of the type $\langle x_i f(\boldsymbol{x})\rangle$, can be obtained as [7]

$$\boxed{\langle x_i f(\boldsymbol{x})\rangle = \sum_m \langle x_i x_m\rangle \left\langle \frac{\partial f}{\partial x_m} \right\rangle,} \tag{3.8}$$

a proof of this theorem is provided in [8].

By definition the process ξ_i is assumed as Gaussian with zero mean, which means that the n-dimensional probability distribution $P_n(\xi_1, t_1; ...; \xi_n, t_n)$ is a multivariate Gaussian distribution. Therefore we can apply the result (3.8) to calculate the second term of equation (3.6).

$$\left\langle \frac{p_i}{m_i}\xi_i \right\rangle = \sum_j \int_{-\infty}^{\infty} dt' \left\langle \xi_i(t)\xi_j(t')\right\rangle \frac{1}{m_i}\left\langle \frac{\partial p_i}{\partial \xi_j} \right\rangle \tag{3.9}$$

Considering the relation

$$\langle \xi_i(t)\xi_j(t')\rangle = 2m_i\gamma_i k_B \tau_i \delta_{ij}\delta(t-t'), \tag{3.10}$$

and the equations of (3.3)

$$dp_i = -\left(\frac{dV_i}{dx_i} + \frac{\partial V_{int}}{\partial x_i} + \gamma_i p_i\right) dt + \xi_i(t)dt = -\left(\frac{dV_i}{dx_i} + \frac{\partial V_{int}}{\partial x_i} + \gamma_i p_i\right) dt + d\xi_i, \tag{3.11}$$

we see that

$$\frac{\partial p_i}{\partial \xi_i} = 1. \tag{3.12}$$

The integral (3.9) takes the form

$$\left\langle \frac{p_i}{m_i}\xi_i \right\rangle = \frac{1}{m_i}\sum_j \int_{-\infty}^{\infty} dt' 2m_i\gamma_i k_B \tau_i \delta_{ij}\delta(t-t') = 2\gamma_i k_B \tau_i. \tag{3.13}$$

Associating the first term with the kinetic temperature (T_i) that is given by the equipartition theorem (A.11) we can write (3.6) as

$$j_i = \gamma_i k_B \left(\tau_i - T_i\right) \tag{3.14}$$

Since the total system is isolated, the heat currents j_1 and j_2 must be equal and of opposite sign. (Figure 3.3)

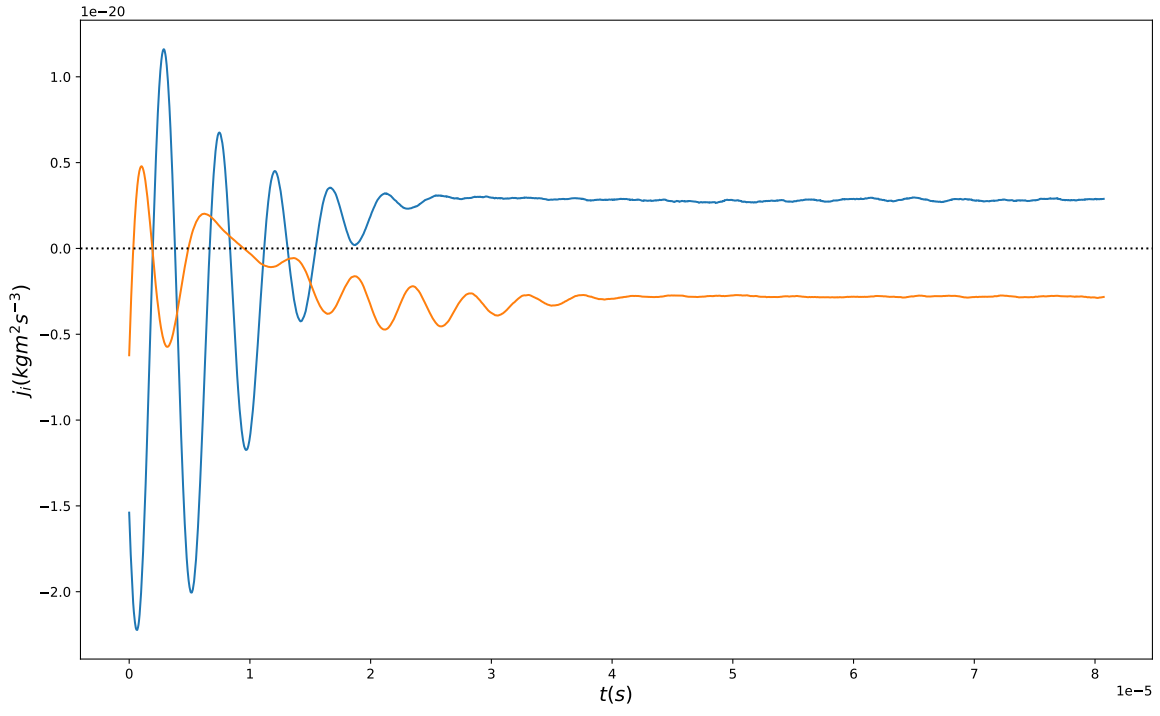

Figure 3.3: Heat currents between bath-1 to particle-1 (blue line) and bath-2 to particle-2 (orange line). The values of the system parameters are the same as in figure 3.2.

The values obtained for the heat currents with (3.14) require that the particle have a well-defined temperature that is given by the equipartition theorem. However the steady state

reached by the system is out of equilibrium so the equipartition theorem should not be valid. This is where the concept of local thermal equilibrium (LTE) comes in, a tool that allows us to generalize results from statistical physics in equilibrium to non-equilibrium systems. The idea is to consider that the total system can be divided into a series of subsystems which are in equilibrium at a certain local temperature. In each of these subsystems all the results of the statistical physics of equilibrium, including the equipartition theorem, are fulfilled in at least an approximate way.

As we saw in the previous chapter, a state of equilibrium is characterized by the distribution of speeds that the particle presents. If the distribution is Maxwellian then we can affirm that our system has reached equilibrium and, as mentioned before, said distribution will have a null value of kurtosis associated with it. So when the particle is in LTE, the velocity distribution must be the same as in equilibrium, that is, its kurtosis must be zero.

In figure 3.4 we can see both the temperature and the kurtosis of the particle "1" at each instant of time. We observe that although the kinetic temperature of the particle reaches stationary values (first blue line) the kurtosis does not stabilize its value at zero until a later instant (second blue line) as we observe in cases in equilibrium. We also see that as in the case of the particle in contact with a single bath at a harmonic potential, the kurtosis profile presents a series of minimum values before stabilizing at zero.

The behavior of both the temperature an the kurtosis is similar for the other particle.

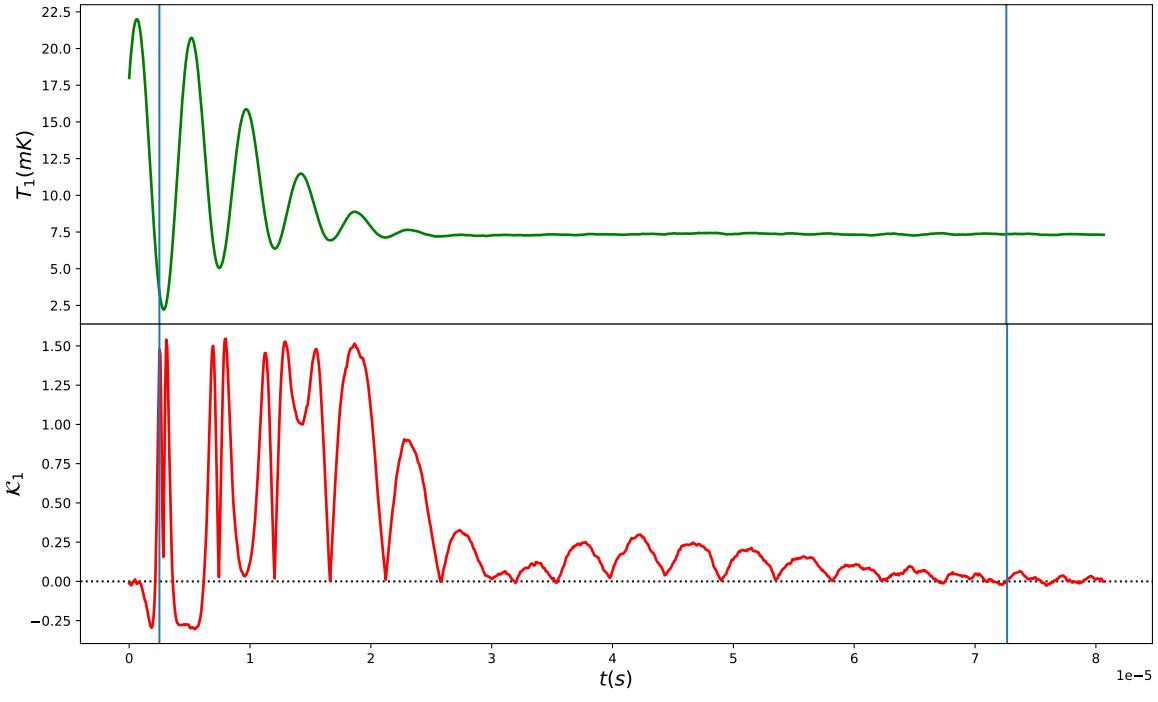

Figure 3.4: Above, the temporal evolution of the kinetic temperature of particle 1. Below, the temporal evolution of the kurtosis associated with the velocity distribution of the same particle. The blue lines are instants for which we represent the velocity distributions. The values of the system parameters are the same as in figure 3.2.

In figure 3.5 the distributions for the instants indicated in figure 3.4 are shown.

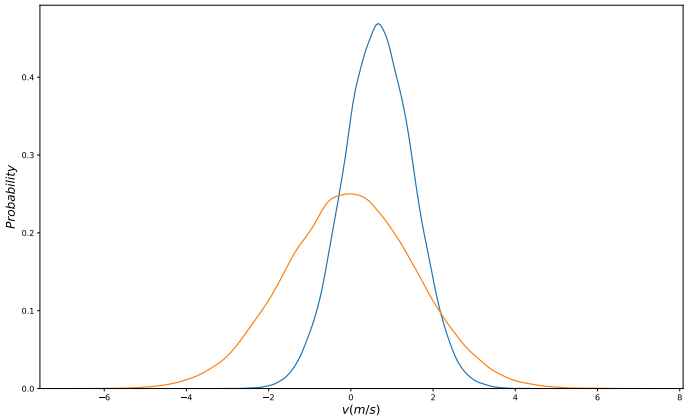

Figure 3.5: The blue distribution corresponds to the blue line on the left (non-LTE) in Figure 3.4 while the orange one corresponds to the one on the right (LTE).

3.1.1 Velocity correlations.

In figure 3.6 all the particle 1 velocity correlations are shown. As in the cases of systems reaching equilibrium, we see that all correlations become zero at a certain point in time.

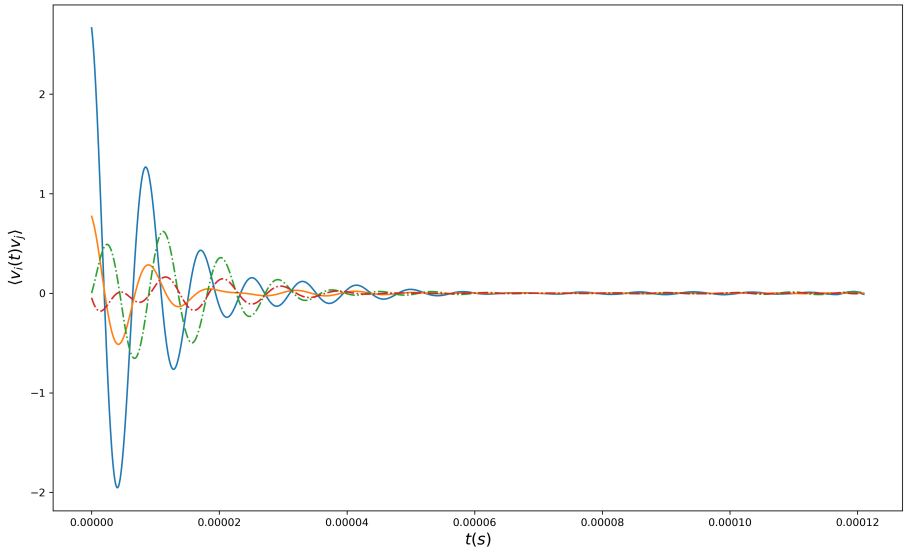

Figure 3.6: Correlations $\langle v_1(t)v_1\rangle$ (blue line), $\langle v_2(t)v_2\rangle$ (orange line), $\langle v_1(t)v_2\rangle$ (green line) and $\langle v_2(t)v_1\rangle$ (red line). The values of the system parameters are the same as in figure 3.2.

Although it is known that for the LTE status to be achieved it is necessary that the correlations have a rapid decay. [3] We have obtained that this time coincides with the time necessary for the kurtosis to be zero in a definitive way.

3.2 Steady state study: Semi-analytical method.

Below is a semi-analytical method that allows us to know the state of the system once the steady state and LTE has been reached. Although the development of the method is carried out for the simplest particular case of the system that is discussed in this chapter, it could be applied to more complex (harmonic) systems.

3.2.1 Method approach.

The Hamiltonian of the system (3.1) can be written for the case $V_1 = 0$ and $V_2 = 0$ in the form

$$H_s = \frac{p_1^2}{2m_1} + \frac{p_2^2}{2m_2} + \frac{k}{2}\left[(x_1 - x_{1e}) - (x_2 - x_{2e})\right]^2, \tag{3.15}$$

with x_{1e} and x_{2e} the equilibrium positions of both particles.

Now we make a change of coordinates to the reference system of the center of mass (Q, P) and relative quantities (q, p). The new coordinates will be

$$\begin{aligned} Q &= \frac{1}{M}(m_1 x_1 + m_2 x_2) \\ P &= p_1 + p_2, \\ q &= x_1 - x_2 - x_e, \\ p &= \mu\left(\frac{p_1}{m_1} - \frac{p_2}{m_2}\right), \end{aligned} \tag{3.16}$$

where $M = m_1 + m_2$, $\mu = (1/m_1 + 1/m_2)^{-1}$ and $x_e = x_{2e} - x_{1e}$.

In this system of coordinates the Hamiltonian (3.15) takes the following form

$$H_s = \frac{P^2}{2M} + \frac{p^2}{2\mu} + \frac{k}{2}q^2. \tag{3.17}$$

The equations of motion for the two particles coupled to the Langevin thermal baths in this frame are given by

$$\begin{aligned} \dot{Q} &= \frac{P}{M}, \\ \dot{q} &= \frac{p}{\mu}, \\ \frac{\dot{P}}{M} &= -\frac{1}{M}(\gamma_1 + \gamma_2)\frac{P}{M} - \frac{\mu}{M}\left(\frac{\gamma_1}{m_1} - \frac{\gamma_2}{m_2}\right)\frac{p}{\mu} + \frac{1}{M}\left(\xi_1(t) + \xi_2(t)\right), \\ \frac{\dot{p}}{\mu} &= -\frac{k}{\mu}q - \left(\frac{\gamma_1}{m_1} - \frac{\gamma_2}{m_2}\right)\frac{P}{M} - \mu\left(\frac{\gamma_1}{m_1^2} + \frac{\gamma_2}{m_2^2}\right)\frac{p}{\mu} + \frac{\xi_1(t)}{m_1} - \frac{\xi_2(t)}{m_2}. \end{aligned} \tag{3.18}$$

The system of equations (3.18) can be expressed in matrix form as

$$\dot{\boldsymbol{R}} = \boldsymbol{A} \cdot \boldsymbol{R} + \boldsymbol{g}(t), \tag{3.19}$$

with

$$\boldsymbol{R} = \left(q, \frac{P}{M}, \frac{p}{\mu}\right)^T,$$

$$\boldsymbol{A} = \begin{pmatrix} 0 & 0 & 1 \\ 0 & -\frac{1}{M}(\gamma_1+\gamma_2) & -\frac{\mu}{M}\left(\frac{\gamma_1}{m_1}-\frac{\gamma_2}{m_2}\right) \\ -\frac{k}{\mu} & -\left(\frac{\gamma_1}{m_1}-\frac{\gamma_2}{m_2}\right) & -\mu\left(\frac{\gamma_1}{m_1^2}+\frac{\gamma_2}{m_2^2}\right) \end{pmatrix}, \tag{3.20}$$

$$\boldsymbol{g}(t) = \left(0, \frac{1}{M}\left(\xi_1(t)+\xi_2(t)\right), \frac{\xi_1(t)}{m_1}-\frac{\xi_2(t)}{m_2}\right)^T,$$

the matrix $\boldsymbol{A}$ is called the dynamic matrix of the system. The coordinate referring to the position of the center of mass Q has not been considered because the system of equations obtained (3.18) is independent of it. By making the change of coordinates we have managed to reduce the problem from 4 dimensions to 3.

The formal solution of (3.19) gives the components of the vector $\boldsymbol{R}$ as

$$R_i(t) = \sum_j V_{ij} \sum_k [\boldsymbol{V}^{-1}]_{ij} \int_{t_0}^{t} e^{r_j(t-s)} g_k(s) ds + \sum_j V_{ij} e^{r_j(t-t_0)} \sum_l [\boldsymbol{V}^{-1}]_{jl} R_l(t_0), \tag{3.21}$$

with t_0 the initial time, and $\boldsymbol{V}$ the matrix with the eigenvectors of matrix $\boldsymbol{A}$ and r_j its corresponding eigenvalues. To see how this result is obtained, you can refer to the bibliography[9]. The covariance matrix in the steady state (ss) can be writen as

$$\langle \boldsymbol{RR} \rangle_{ss} = \boldsymbol{V} \cdot \boldsymbol{J} \cdot \boldsymbol{V}^T, \tag{3.22}$$

where $\boldsymbol{J}$ is the matrix with elements

$$J_{ij} = \frac{[J_A]_{ij}}{r_i r_j} - \frac{[J_B]_{ij}}{(r_i + r_j)}. \tag{3.23}$$

with the matrices $\boldsymbol{J}_A = \boldsymbol{V}^{-1} \cdot \boldsymbol{G}_A \cdot (\boldsymbol{V}^{-1})^T$ and $\boldsymbol{J}_B = \boldsymbol{V}^{-1} \cdot \boldsymbol{G}_B \cdot (\boldsymbol{V}^{-1})^T$. The two matrices $\boldsymbol{G}_A$ and $\boldsymbol{G}_B$ arise from the autocorrelation of the vector $\boldsymbol{g}(t)$, given by

$$\langle \boldsymbol{g}(t)\boldsymbol{g}(t') \rangle = \begin{pmatrix} 0 & 0 & 0 \\ 0 & \frac{2k_B}{M^2}(\gamma_1\tau_1+\gamma_2\tau_2)\delta(t-t') & \frac{2k_B}{M}\left(\frac{\gamma_1\tau_1}{m_1}-\frac{\gamma_2\tau_2}{m_2}\right)\delta(t-t') \\ 0 & \frac{2k_B}{M}\left(\frac{\gamma_1\tau_1}{m_1}-\frac{\gamma_2\tau_2}{m_2}\right)\delta(t-t') & 2k_B\left(\frac{\gamma_1\tau_1}{m_1^2}+\frac{\gamma_2\tau_2}{m_2^2}\right)\delta(t-t') \end{pmatrix} = \boldsymbol{G}_A + \boldsymbol{G}_B \delta(t-t'). \tag{3.24}$$

3.2.2 Numerical simulations.

We analyze a system composed of two masses $m_1 = 6.65 \times 10^{-26}(kg)$ and $m_2 = 4.03 \times 10^{-26}(kg)$, like before, with different values of the strenght of the inter-particle harmonic interaction k.

We consider that the two-particle system is coupled to a hot thermal reservoir with temperature $\tau_h = 9mK$ and to a cold one with temperature $\tau_c = 3mK$. We will study how heat currents and temperatures behave in the steady state for a given arrangement of hot and cold baths. We will study how heat currents and temperatures behave in the steady state for a given arrangement of hot and cold baths. Then we carry out the same study but inverting the arrangement of the baths to observe if the thermal transport in the system depends on the sign of the temperature gradient that is if our system presents thermal rectification. [10]

Temperatures and energy current as a function of γ_1.

We fix the friction coefficient that characterize the interaction with the second reservoir 2 at $\gamma_2 = 5 \times 10^{-21} kg/s$. While we change the coupling to the first reservoir 1 by considering values of the friction coefficient γ_1 in the interval $(5 \times 10^{-23}, 2 \times 10^{-20}) kg/s$.

Figure 3.7 shows the steady temperatures T_1 and T_2 as a function of γ_1 for different values of the strenght of the inter-particle harmonic interaction k. Figure 3.8 shows the same for the energy current j_1. The steady state temperatures T_1 and T_2 corresponding to the forward and reversed thermal reservoir configurations are symmetric, with the mirror line at the average temperature $\tau_m = (\tau_1 + \tau_2)/2$. Whereas the exchange of the two thermal reservoirs leads to an inversion in the direction of the steady state energy current j_1, but it does not modify its magnitude. Thus, the thermal rectification is absent, indepently of the values of the model parameters.

Temperatures and energy current as a function of k.

Here we fix the friction coefficient $\gamma_2 = 5 \times 10^{-21} kg/s$ and set different values of γ_1. While we consider values of the strength of the inter-particle harmonic interaction k in the interval $(1 \times 10^{-17}, 1 \times 10^{-13}) kg/s^2$.

Figure 3.9 shows the steady temperatures T_1 and T_2 as a function of k for different values of friction coefficient γ_1. As expected, for very small values of k each particle reachs the temperature of the thermal reservoir in which its is immersed, we retrieve the results from chapter 2. While in the limit of very strong coupling the steady temperatures take a constant value which is independent of k.

Here again he exchange of the two thermal reservoirs leads to the inversion of the temperatures around the mirror line at τ_m. Also, the analysis of the energy current j_1 indicates the absence of thermal rectification (Figure 3.10). The forward and reversed thermal reservoir configurations present energy currents in opposite direction, but with identical magnitude.

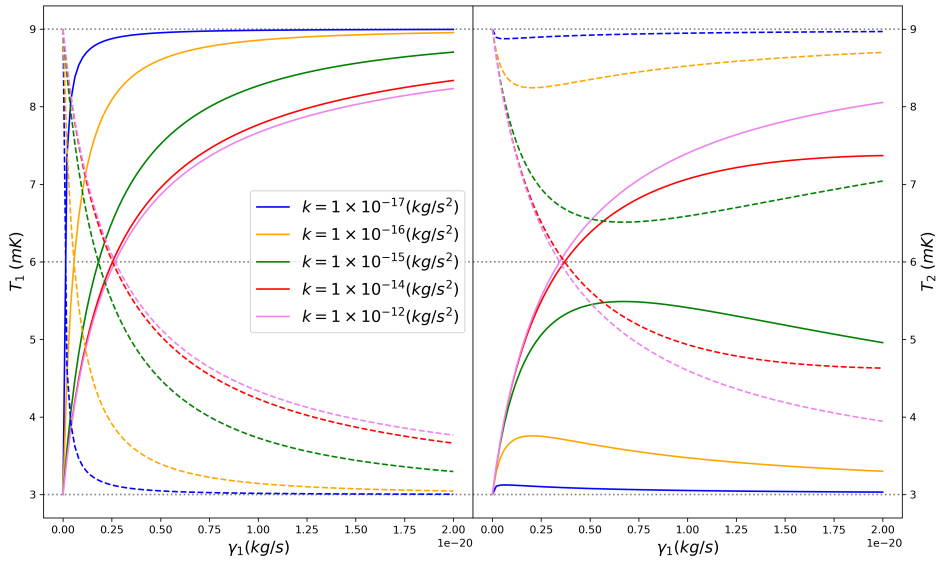

Figure 3.7: The steady state kinetic temperatures T_1 (left) and T_2 (right) as a function of the friction cofficient γ_1, for different values of the strenght of the inter-particle harmonic interaction k. The blue line corresponds to $k = 1 \times 10^{-17} kg/s^2$, the yellow line to $k = 1 \times 10^{-16} kg/s^2$, the green line to $k = 1 \times 10^{-15} kg/s^2$, the red line to $k = 1 \times 10^{-14} kg/s^2$ and the rose line to $k = 1 \times 10^{-12} kg/s^2$. The solid lines correspond to the thermal reservoir configuration given by $\tau_1 = \tau_h = 9mK$ and $\tau_2 = \tau_c = 3mK$, and the dotted lines to the reverse configuration. The black horizontal dotted lines give the temperatures τ_h and τ_c of the two thermal reservoirs, and their average τ_m.

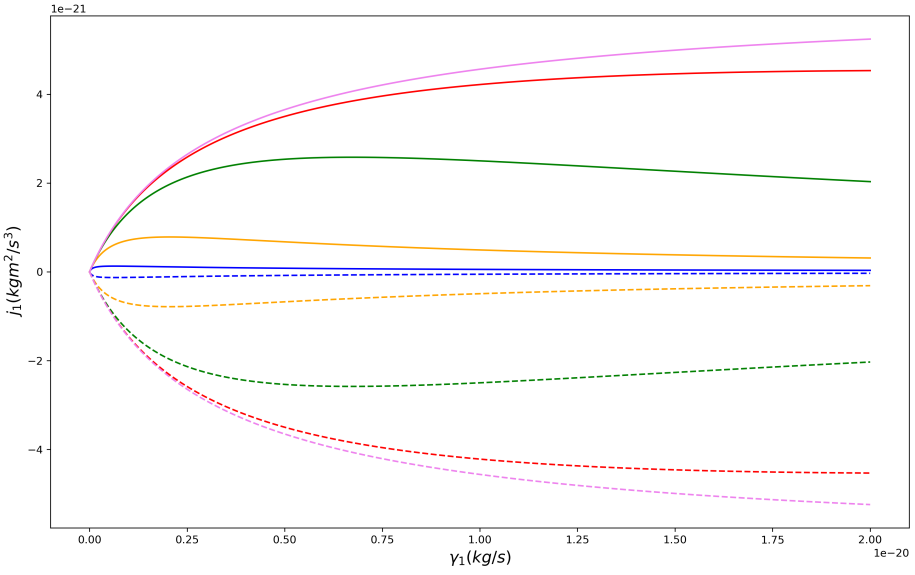

Figure 3.8: The steady state energy current j_1 coming from the left thermal reservoir into the particle 1, as a function of the friction cofficient γ_1, for different values of the strenght of the inter-particle harmonic interaction k. The color code for the different values of k is the same as in Figure 3.5. The solid lines correspond to the thermal reservoir configuration given by $\tau_1 = \tau_h = 9mK$ and $\tau_2 = \tau_c = 3mK$, and the dotted lines to the reverse configuration.

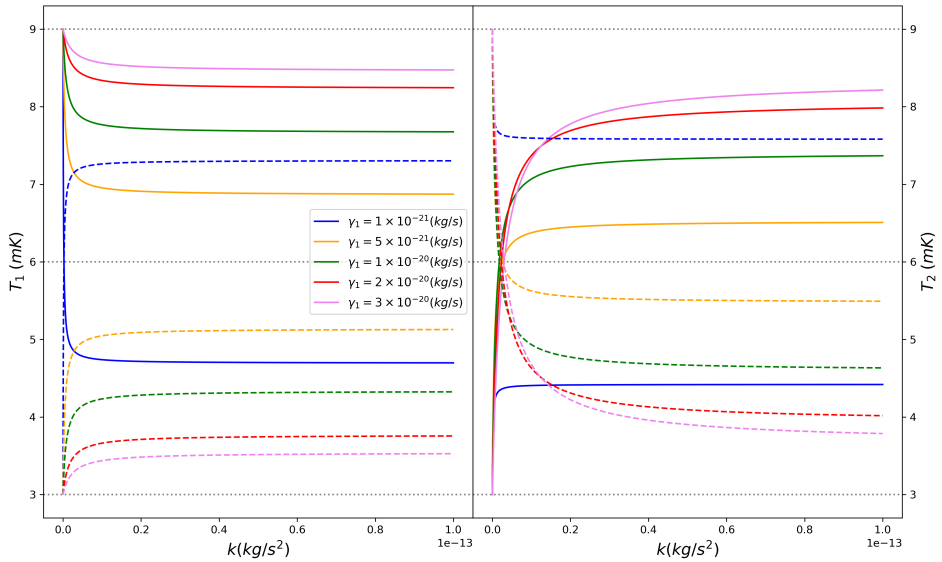

Figure 3.9: The steady state temperatures T_1 (left) and T_2 (right) as a function of the strenght of the inter-particle harmonic interaction k, for different values of the friction coefficient γ_1. The blue line corresponds to $\gamma_1 = 1 \times 10^{-21} kg/s$, the yellow line to $\gamma_1 = 5 \times 10^{-21} kg/s$, the green line to $\gamma_1 = 1 \times 10^{-20} kg/s$, the red line to $\gamma_1 = 2 \times 10^{-20} kg/s$ and the rose line to $\gamma_1 = 3 \times 10^{-20} kg/s$. The solid lines correspond to the thermal reservoir configuration given by $\tau_1 = \tau_h = 9mK$ and $\tau_2 = \tau_c = 3mK$, and the dotted lines to the reverse configuration. The black horizontal dotted lines give the temperatures τ_h and τ_c of the two thermal reservoirs, and their average τ_m.

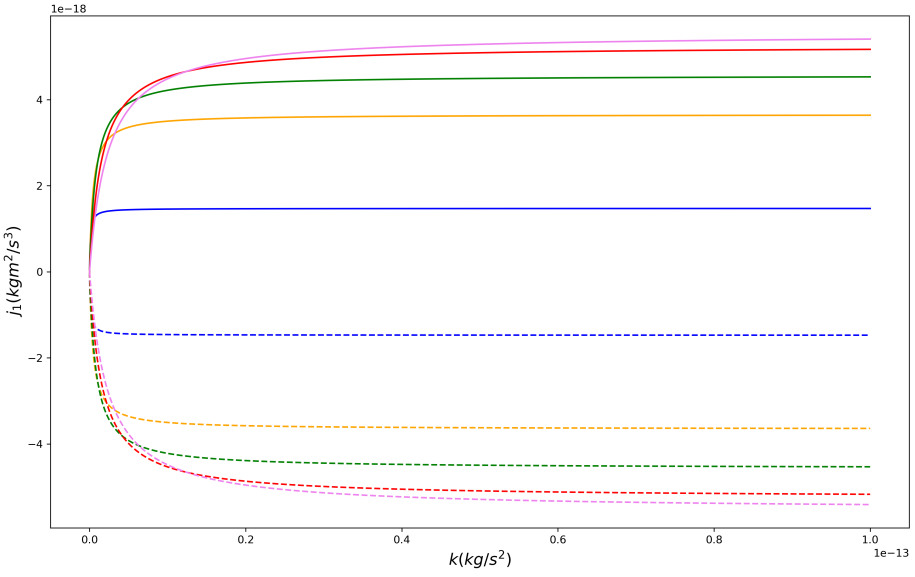

Figure 3.10: The steady state energy current j_1 coming from the left thermal reservoir into the particle 1, as a function of the strenght of the inter-particle harmonic interaction k, for different values of the friction coefficient γ_1. The color code for the different values of k is the same as in Figure 3.5. The solid lines correspond to the thermal reservoir configuration given by $\tau_1 = \tau_h = 9mK$ and $\tau_2 = \tau_c = 3mK$, and the dotted lines to the reverse configuration.

Conclusions.

About Brownian motion and the Langevin model.

In Chapter 1 a mathematical description of Brownian motion is carried out starting from the concept of stochastic process. From the result obtained by Einstein and shown in Appendix A, we connect with the need to define these processes with normal probability distributions when we want to describe Brownian motion. With this we introduce the Central Limit Theorem. Once the displacement of the particle had been fully described, we went on to discuss how to model the action of the thermal bath and for this the Langevin equations were introduced. The chapter ends with a description of the hypotheses carried out to model the Langevin force, leaving the ground prepared for the introduction of the Fluctuation-Dissipation Theorem that will appear naturally when the case of the free particle is studied in the second chapter. In this sense, chapter one is presented as a light but comprehensive introduction to Brownian motion from early beginnings.

The second chapter has three functions. Firstly, it allows us to obtain results of great theoretical interest that allow us to better understand the behavior of systems in equilibrium that can then be extrapolated to systems in non-equilibrium. Since in the latter, obtaining analytical solutions becomes impossible in most cases. It also allows us to introduce methods for solving the equations of motion, such as Harmonic Analysis. Last but probably most important, we obtain solutions to test the convergence of the numerical results of our simulations. This way we check that they work correctly before moving on to study out-of-equilibrium systems.

About the study of non-equilibrium states.

Firstly, we verify that the presence of more than one bath forces the particle to stabilize its temperature without achieving thermalization at the temperature of its bath, proving that a non-equilibrium state is reached.

We observe that, as in equilibrium systems, the mean values of the velocities decay to zero. Therefore the velocity correlations fully represent the dynamics of the system in the steady state of non-equilibrium. This result seems analogous to that obtained in chapter two but for out-of-equilibrium systems. This is a consequence of the fact that in LTE the results obtained for systems in equilibrium are valid (at least in an approximate way).

Then we characterize the heat currents that appear in the system due to the presence of thermal baths at different temperatures. To do this, we use a mathematical result that plays a central role in the Statistical Mechanics of Non-equilibrium, Novikov's theorem. With this result and our simulations, we obtained the temporal evolution of the currents until reaching the stationary regime. We verify that as the total system is isolated, both currents have the same magnitude but opposite sign once the state of non-equilibrium steady state is reached.

About kurtosis and LTE conditions.

We observe that in systems that don't conserve linear momentum, the kurtosis profile presents a series of minima in which they become zero before a steady state or equilibrium is reached. This could be that the system goes through a series of LTE states before reaching its final state and can be related to studies which states that the non-conservation of linear momentum in systems of reduced dimensionality is the reason why anomalous transport phenomena don't appear (and therefore the existence of LTE) [11]. Although momentum conservation seems to be a fundamental aspect so that the system does not deviate from LTE, there are studies that show systems in which the linear momentum is conserved satisfying the Fourier type laws as indicated in [12]. Therefore, in order to get something clear from this result, it would be necessary to do our simulations with a larger number of particles.

A condition analogous to null kurtosis is that the particle velocity correlations decay to zero quickly as we said in Chapter 3. This is consistent with our results. In addition to this, we have observed that said decay time coincides with that of kurtosis. It would be interesting to check if this is generally true for larger systems with more complex interactions. Since doing the study in terms of the correlations of the velocity between particles is more expensive computationally than studying kurtosis.

Another behavior that we observe in all the kurtosis profiles is that they first go through a series of negative values until they finally change to a positive sign. In simulations carried out by [3] this coincides with the moment in which the increase in energy of the particle $\Delta E = \langle E \rangle(t) - E_0$ reached its maximum value. This result is verified in the figure 3.10.

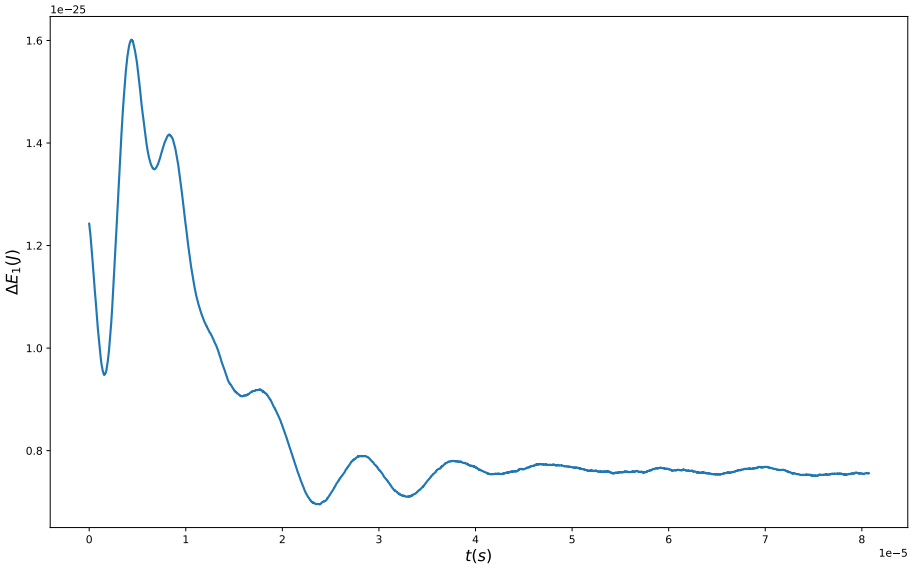

Figure 3.11: Energy of the particle 1. The values of the system parameters are the same as in figure 3.2.

No clear reason for this has been found in the scientific literature.

About the semi-analytic method and the thermal rectification.

Although through simulations we can obtain the values of temperature and heat currents in the steady state of non-equilibrium, this is computationally demanding. An alternative is to verify that the steady state of non-equilibrium is in LTE by means of a kurtosis study and then use the semi-analytical method described in Chapter 3 which requires much less computing power. In this way, it is possible to study quite complex harmonic systems with limited computing power.

On the other hand, with the study carried out using this method, no thermal rectification was observed for any type of configuration of the system parameters. This could be due to the fact that the system is under the action of a harmonic potential. Some studies relate thermal rectification with the presence of asymmetries associated with non linear interaction in the system. [13]

Bibliography

[1] Pierre Gaspard. *Nonequilibrium nanosystems*. Université Libre de Bruxelles, 2010.

[2] Roberto Livi and Stefano Lepri. Heat in one dimension. *Nature*, 421:327, 2003.

[3] Lei Wang. Validity of local thermal equilibrium in anomalous heat diffusion. *New Journal of Physics*, 21, 2019.

[4] R. Kubo. *Statistical Physics II. Nonequilibrium Statistical Mechanics*. Springer, 1991.

[5] Giorgio Volpe and Giovanni Volpe. Simulation of a brownian particle in an optical trap. *American Journal of Physics*, 81:224, 2012.

[6] N. Pottier. *Nonequilibrium Statistical Physics*. Oxford University Press, 2010.

[7] E. A. Novikov. Functionals and the random-force method in turbulence theory. *Soviet Physics JETP*, 20, 1964.

[8] J. L. García-Palacios. *Introduction to the theory of stochastic processes and Brownian motion problems*. Universidad de Zaragoza, 2004.

[9] Richard C. DiPrima and William E. Boyce. *Elementary Differential Equations*. John Wiley Sons Ltd; 9th Revised edition, 2008.

[10] N.A. Roberts and D.G. Walker. *A Review of Thermal Rectification Observations and Models in Solid Materials*. Department of Mechanical Engineering, Vanderbilt University, Nashville.

[11] Abhishek Dhar. Heat transport in low-dimensional systems. *Advances in Physics*, 00:1–78, 2008.

[12] Mark Buchanan. Heated debate in different dimensions. *Nature Physics*, 1:71, 2005.

[13] Nan Zeng. Mechanisms causing thermal rectification: The influence of phonon frequency, asymmetry, and nonlinear interactions. *Physical Review B*, 78, 2008.

Appendix A

Einstein's solution to the Brownian motion.

Although Robert Brown's observations were carried out in 1827, an explanation for the Brownian motion was not developed until 1905 when Albert Einstein published an article entitled "Concerning the motion, as required by the molecular-kinetic theory of heat, of particles suspended in liquids at rest ".

There are two main points on which Einstein's solution was based:

1- the movement is caused by extremely frequent collisions of the pollen grains with the molecules in incessant movement of the liquid in which they are suspended.

2- the movement of these molecules is extremely complicated and therefore their effect on the pollen grain can only be described in a probabilistic way in terms of statistically independent impacts that occur with great frequency.

To repeat the derivation carried out by Einstein we define the time interval τ, small enough compared to the observation times but large enough so that the dynamics of the particle once elapsed τ can be considered independent of the one that followed when you began to measure time.

A number$n$ of particles suspended above the liquid is assumed. In the course of a time interval τ the coordinates of the particles will experience a change Δ that can be positive or negative indistinctly for each particle. The number of dn particles that will experience an increase between Δ and $\Delta + d\Delta$ will be given by an expression as follows:

$$dn = n\phi(\Delta)d\Delta \tag{A.1}$$

where $\phi(\Delta)$ could be interpreted as the probability that a particle experiences a particular Δ displacement. Therefore, it must fulfill the condition that $\int_{-\infty}^{\infty} \phi(\Delta)d\Delta = 1$, it must also have non-zero values only for small Δ and satisfy the condition of being an even function i.e $\phi(-\Delta) = \phi(\Delta)$.

We will now study the dependence of the diffusion coefficient on phi, restricting ourselves to the case in which the number of particles per unit volume only depends on the variables x and t.

Let's call the particle volumetric density function $f(x,t)$. Now we calculate the particle distribution at time $t + \tau$ from the distribution at time t. Using the definition of ϕ we can express the number of particles between two planes perpendicular to the X axis that pass through x and $x + dx$ as:

$$f(x, t+\tau)dx = dx \int_{-\infty}^{\infty} f(x+\Delta, t)\phi(\Delta)d\Delta \tag{A.2}$$

Equation 2 is called the Chapman – Kolgomorov equation and can be interpreted as that the probability of finding the particle at a point x at a time $t+\tau$ is given by the sum of all the probabilities of all the possible displacements Δ from positions $x+\Delta$ multiplied by the probability of being at a point $x+\Delta$ at a time t. This is based on the consideration that the displacement Δ is independent of the previous movement of the particle.

Since τ is small we can write the left member of (2) as:

$$f(x, t+\tau) = f(x, t) + \tau\frac{\partial f}{\partial t}$$

then it is also possible to expand the right side in powers of Δ:

$$f(x+\Delta, t) = f(x, t) + \Delta\frac{\partial f}{\partial x} + \frac{\Delta^2}{2!}\frac{\partial^2 f}{\partial x^2} + ...$$

Taking all this to equation (2) we obtain:

$$f(x,t) + \tau\frac{\partial f}{\partial t} = f(x,t)\int_{-\infty}^{\infty}\phi(\Delta)d\Delta + \frac{\partial f}{\partial x}\int_{-\infty}^{\infty}\Delta\phi(\Delta)d\Delta + \frac{\partial^2 f}{\partial x^2}\int_{-\infty}^{\infty}\frac{\Delta^2}{2!}\phi(\Delta)d\Delta + ... \tag{A.3}$$

since ϕ is a function for the integrals 2,4, ... on the right side of the equality are zero while the integrals 1,3,5 ... are getting smaller and smaller. Therefore, considering only the integrals 1 and 3 in addition to the condition that ϕ is normalized and identifying the diffusion coefficient (D) as:

$$D = \frac{1}{\tau}\int_{-\infty}^{\infty}\frac{\Delta^2}{2}\phi(\Delta)d\Delta$$

we arrive at the diffusion equation of the form:

$$\frac{\partial f}{\partial t} = D\frac{\partial^2 f}{\partial x^2} \tag{A.4}$$

Which is known as the Fokker – Planck equation, an equation in partial derivatives of the parabolic type.

The conditional probability $f(x_0, t_0|x, t)$ is the fundamental solution of this equation for the initial condition

$$f(x_0, t_0|x, t) = \delta(x - x_0)$$

and is given by [4]

$$f(x_0, t_0|x, t) = \frac{1}{\sqrt{4\pi D(t-t_0)}}exp\left(-\frac{(x-x_0)}{4D(t-t_0)}\right) \tag{A.5}$$

Appendix B

Demonstration of the Central Limit Theorem.

We know that any characteristic function with null mean and standard deviation σ^2 will fulfill

$$G_X(k) = \int dx e^{ikx} P_X(x) = 1 - \frac{1}{2}\sigma^2 k^2 + ... \tag{B.1}$$

For a random variable $Y = X_1 + ... + X_n$ the following relation is satisfied

$$G_Y(k) = \int dx_1 ... \int dx_n e^{ik(X_1+...+X_n)} P_{X_1...X_2}(x_1, ..., x_n) = \prod_i^n G_{X_i}(k) = [G_X(k)]^n, \tag{B.2}$$

to get to the last expression we assume that all variables have equivalent statistical properties. Now we consider a variable of the form $Z = Y/\sqrt{n}$ such that

$$\lim_{n\to\infty} G_Z(k) = \lim_{n\to\infty} G_Y\left(\frac{k}{\sqrt{n}}\right) = \lim_{n\to\infty}\left[G_X\left(\frac{k}{\sqrt{n}}\right)\right]^n \simeq \left(1 - \frac{\sigma^2 k^2}{2n}\right)^2 \to exp(-\frac{1}{2}\sigma^2 k^2) \tag{B.3}$$

The last expression in (B.3) coincides with the characteristic function of a Gaussian. As it was wanted to demonstrate.[8]

Appendix C

Numerical integration. Platen's algorithm.

We consider a particle of mass m, with position $x(t)$ and momentum $p(t)$, which is under the action of a potential $V(x)$ and in contact with a thermal bath at a temperature T. For this case the Langevin equations are of the form (2.1). Taking into account the condition (1.22) for the mean value of the Langevin force and the expression for the autocorrelation of the force taking into account the fluctuation-dissipation theorem (2.15).

The equations of motion can be rewritten in the form

$$\begin{aligned} dx &= \frac{p}{m}dt \\ dp &= -\left(\frac{\partial V}{\partial x} + \gamma p\right)dt + \sqrt{2m\gamma k_B T}dw, \end{aligned} \tag{C.1}$$

where dw corresponds to a set of independent random numbers that satisfies a Gaussian distribution. Considering the vector

$$\boldsymbol{y}(t) = \begin{pmatrix} x(t) \\ p(t) \end{pmatrix}. \tag{C.2}$$

The equations of motion in matrix form are given

$$d\boldsymbol{y} = \boldsymbol{A}(\boldsymbol{y})dt + \tilde{\boldsymbol{B}} \cdot d\boldsymbol{W}, \tag{C.3}$$

with the vector $\boldsymbol{A}(\boldsymbol{y})$ being

$$\boldsymbol{A}(\boldsymbol{y}) = \begin{pmatrix} \dfrac{p}{m} \\ -\dfrac{\partial V}{\partial x} - \gamma p \end{pmatrix}, \tag{C.4}$$

and the matrix $\tilde{\boldsymbol{B}}$

$$\tilde{\boldsymbol{B}} = \begin{pmatrix} 0 & 0 \\ 0 & \sqrt{2m\gamma k_B T} \end{pmatrix}. \tag{C.5}$$

For the vector containing the random numbers we have

$$d\boldsymbol{W} = \begin{pmatrix} 0 \\ dw \end{pmatrix}. \tag{C.6}$$

Given an initial time t_0 for which we know the initial position and velocity of the particle

$$\boldsymbol{y}(t_0) = \begin{pmatrix} x(t_0) \\ p(t_0) \end{pmatrix} = \begin{pmatrix} x_0 \\ p_0 \end{pmatrix}, \tag{C.7}$$

our goal is to determine their values at a later time $t_f > t_0$. We want to know

$$\boldsymbol{y}(t_f) = \begin{pmatrix} x(t_f) \\ p(t_f) \end{pmatrix}. \tag{C.8}$$

To perform the numerical integration of the equations of motion, we consider a discretization of the time interval (t_0, t_f), in a sufficiently large number N_t intervals of the type (t_i, t_{i+1}) of the same size, as seen in figure C.1.

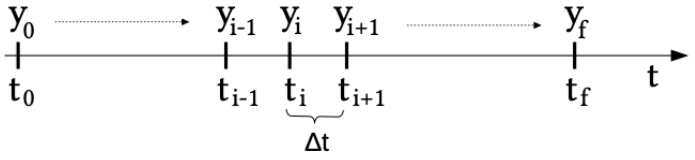

Figure C.1: Discretization of the time interval.

Taking this into account, we assume that said time step between two consecutive time intervals is constant. This is

$$\Delta t = t_{i+1} - t_i = cte. \tag{C.9}$$

For Platen's algorithm, given the variable $\boldsymbol{y}_i = \boldsymbol{y}(t_i)$ in a time step $t = t_i$, its value in t_{i+1} will be given by

$$\boxed{\boldsymbol{y}_{i+1} = \boldsymbol{y}_i + \frac{1}{2}\left[\boldsymbol{A}(\boldsymbol{z}_i) + \boldsymbol{A}(\boldsymbol{y}_i)\right]\Delta t + \tilde{\boldsymbol{B}} \cdot d\boldsymbol{W}_i}, \tag{C.10}$$

with the vector $\boldsymbol{z}_i$ is given by

$$\boldsymbol{z}_i = \boldsymbol{y}_i + \boldsymbol{A}(\boldsymbol{y}_i)\Delta t + \tilde{\boldsymbol{B}} \cdot d\boldsymbol{W}_i \tag{C.11}$$

and

$$d\boldsymbol{W}_i = \sqrt{\Delta t} G_i. \tag{C.12}$$

where G_i is a random variable that satisfies a Gaussian distribution with zero mean and unit variance. This variableG_i by means of a Python random number generator (Although algorithms such as Box-Muller could be used).

Numerical obtaining of statistical averages.

Let $f(t)$ be a statistical process that evolves in time from a well-defined initial value. The average of said process at a given time can be obtained from an average over a sufficiently large number of trajectories that correspond to said process. In figure C.2 it can be seen that the trajectories start from the same initial value.

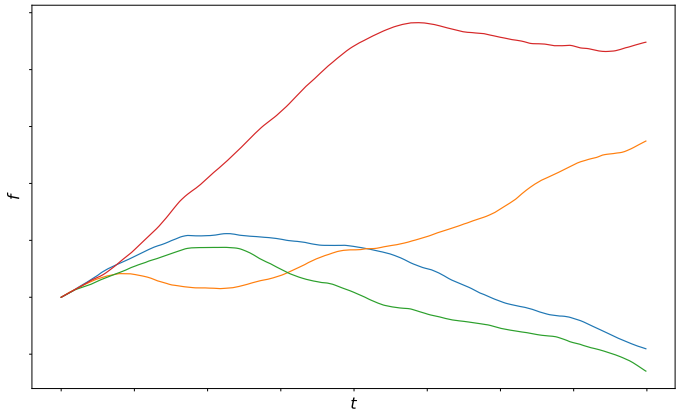

Figure C.2: Temporal evolution of different trajectories corresponding to the stochastic process $f(t)$.

Said stochastic average is then defined as

$$\langle f \rangle(t) = \frac{1}{N} \sum_{i=1}^{N} f_i(t). \tag{C.13}$$

For the statistical average to be valid, the number N must be large enough. In turn, the number of time steps N_t required to achieve good convergence of the results must also be of a high value. Due to this, the storage in memory of the data corresponding to the totality of the trajectories in every time step, to calculate the statistical average, does not make sense. The simple strategy shown here that avoids the need to store an excessive number of data is to store only the average result, and add the new trajectories to that average sequentially.

The average obtained when adding a new trajectory can be expressed in the form

$$\langle f_{N+1} \rangle(t) = \frac{1}{N+1} \left[\sum_{i=1}^{N} f_i(t) + f_{N+1}(t) \right]. \tag{C.14}$$

But taking into account that we can write the first term as

$$\sum_{i=1}^{N} f_i(t) = N \langle f_N \rangle(t). \tag{C.15}$$

Then the average over the $N+1$ paths will be

$$\langle f_{N+1} \rangle(t) = \frac{1}{N+1} \left[N \langle f_N \rangle(t) + f_{N+1}(t) \right]. \tag{C.16}$$

In this way we only store one trajectory in memory.